

Review

Novel Nanocomposite Materials for Advanced Li-Ion Rechargeable Batteries

Chuan Cai and Ying Wang *

Department of Mechanical Engineering, Louisiana State University, Baton Rouge, LA 70803, USA

* Author to whom correspondence should be addressed: E-mail: ywang@me.lsu.edu;
Tel. +1-225-578-8577; Fax: +1-225-578-5924.

Received: 12 August 2009; in revised form: 30 August 2009 / Accepted: 2 September 2009 /
Published: 3 September 2009

Abstract: Nanostructured materials lie at the heart of fundamental advances in efficient energy storage and/or conversion, in which surface processes and transport kinetics play determining roles. Nanocomposite materials will have a further enhancement in properties compared to their constituent phases. This Review describes some recent developments of nanocomposite materials for high-performance Li-ion rechargeable batteries, including carbon-oxide nanocomposites, polymer-oxide nanocomposites, metal-oxide nanocomposites, and silicon-based nanocomposites, etc. The major goal of this Review is to highlight some new progress in using these nanocomposite materials as electrodes to develop Li-ion rechargeable batteries with high energy density, high rate capability, and excellent cycling stability.

Keywords: lithium-ion battery; nanocomposites; cathode; anode

Contents

1. Introduction

2. Nanosized Coatings on Cathode Materials

2.1. Nanosized coatings on lithium transition metal oxides

2.2. Nanosized coatings on lithium phosphates

3. Nanostructured Composites as Cathode Materials

- 3.1. *Nanostructured carbon-oxide composites*
- 3.2. *Nanostructured polymer-oxide composites*
- 3.3. *Nanostructured metal-oxide composites and other nanocomposites*

4. Nanostructured Composite as Anode Materials

- 4.1. *Nanostructured silicon-carbon composites*
- 4.2. *Nanostructured tin-carbon composites*
- 4.3. *Nanostructured tin oxide-carbon composites*
- 4.4. *Nanostructured transition metal oxide-carbon composites*
- 4.5. *Other nanostructured composites*

5. Concluding Remarks

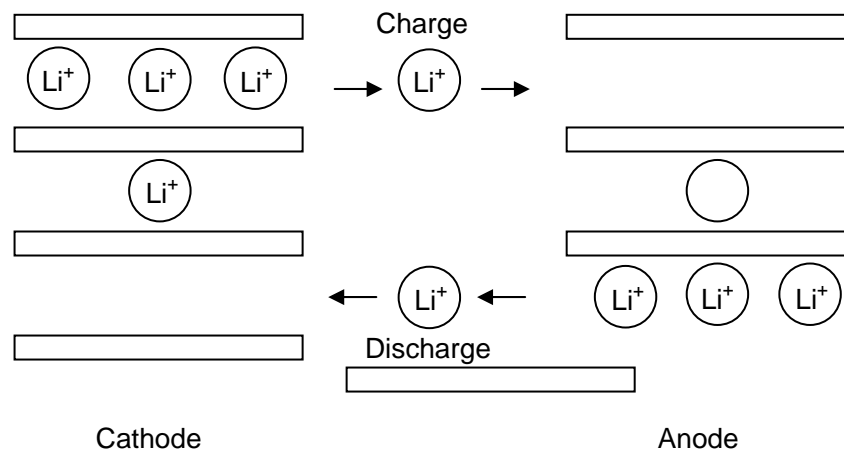
1. Introduction

Recent increases in demand for oil, associated price increases, and environmental issues are continuing to exert pressure on an already stretched world energy infrastructure. One alternative energy/power source under serious consideration is electrochemical energy production, as long as this energy consumption is designed to be more sustainable and more environmentally benign. The lithium-ion battery is the representative system for such electrochemical energy storage and conversion. At present lithium-ion batteries are efficient, light-weight and rechargeable power sources for consumer electronics, such as laptop computers, digital cameras and cellular phones [1]. Moreover, they have been intensively studied for use as power supplies of electric vehicles (EVs) and hybrid electric vehicles (HEVs). High energy and high power densities are required for such devices. Lithium-ion batteries are attractive power-storage devices owing to their high energy density [2]. However, their power density is relatively low because of a large polarization at high charging-discharging rates. This polarization is caused by slow lithium diffusion in the active material and increases in the resistance of the electrolyte when the charging-discharging rate is increased. To solve these problems, it is important to design and fabricate nanostructured electrode materials that provide high surface area and short diffusion paths for ionic transport and electronic conduction.

The principal concept of lithium-ion batteries is illustrated in Figure 1. A combination of a negative lithium intercalation material (anode) with another lithium intercalation material (cathode) having a more positive redox potential gives a Li-ion transfer cell. Anode and cathode are separated by the electrolyte which is an electronic insulator but a Li-ion conductor. Upon charging, lithium ions are released by the cathode and intercalated at the anode. When the cell is discharged, lithium ions are extracted by the cathode and inserted into the anode. Electrode materials must fulfill three fundamental requirements to reach the goal of a high specific energy and energy density: (1) a high specific charge and charge density, *i.e.*, a high number of available charge carriers per mass and volume unit of the material; (2) a high cell voltage, resulting from a high (cathode) and low (anode) standard redox potential of the respective electrode redox reaction; and (3) a high reversibility of electrochemical

reactions at both cathodes and anodes to maintain the specific charge for hundreds of charge/discharge cycles.

Figure 1. Schematic illustration of a lithium-ion battery.



Nanomaterials offer the unusual mechanical, electrical and optical properties endowed by confining the dimensions of such materials. The overall behavior of nanomaterials exhibit combinations of bulk and surface properties [3]. The reports on the processing, properties and applications of nanomaterials are rapidly appearing on daily basis. It is clear that nanostructured electrodes offer improved energy storage capacity and charge/discharge kinetics, as well as better cyclic stabilities due to their huge surface area for Faradaic reaction, and short distance for mass and charge diffusion, as well as the added freedom for volume change during the Li-ion intercalation/deintercalation process.

On the other hand, nanostructured electrodes also introduce new challenges. For example, nanoparticles of LiCoO_2 and LiNiO_2 can react with the electrolyte; nanoparticles of LiMn_2O_4 can dissolve in the electrolyte during cycling. The problems of poor electric conductivity of some cathode materials (e.g., LiFePO_4 , MnO_2 , SnO_2 , TiO_2) and the issues of drastic volume change of some anode materials (e.g., Si, Sn) during cycling cannot be solved by only downsizing the materials to the nanoscale. In addition, nanoparticles of electrode materials tend to agglomerate, resulting in less surface area and reduced electrochemical activity. One solution to these problems is to employ nanocomposites as electrode materials, since nanocomposite materials show even better properties than the constituent components. Typically, composite electrode materials can be prepared by depositing surface coatings on the active materials, dispersing active materials in the host matrices, or adding inactive materials into the active materials. The surface coating on the electrode material serves as a protection layer to hinder the undesirable side reactions with the electrolyte or the dissolution of the active material. Dispersing the electrode material in the host matrix will introduce more freedom for volume change during cycling and hinder the agglomeration of the electrode material. Adding nanosized conductive materials into the electrode material can facilitate the diffusion of Li ions or improve the electronic conductivity and morphological stability.

This article aims to provide a useful survey of recent progress on synthesis and characterizations of nanocomposite electrode materials for lithium-ion batteries. We will start with discussions on nanosized coating on some cathode materials such as lithium transition metal oxides and lithium

phosphates in Section 2. Sections 3 and 4 cover the nanocomposite cathode materials and nanocomposite anode materials, respectively. Each section includes a variety of nanocomposite materials such as carbon-oxide nanocomposites, polymer-oxide nanocomposites, and metal-oxide nanocomposites as cathode materials, and silicon-based, tin-based, and transition metal oxides-based nanocomposites as anode materials.

2. Nanosized Coatings on Cathode Materials

2.1. Nanosized coatings on lithium transition metal oxides

It should be noted that the nanoparticulate forms of lithium transition metal oxides such as LiCoO_2 , LiNiO_2 , or their solid solutions, can react with the electrolyte and cause safety problems. In the case of LiMn_2O_4 , the use of nanoparticles causes undesirable dissolution of Mn. Better stability can be achieved by coating the electrode materials with a nanosized stabilizing surface layer that alleviates these problems.

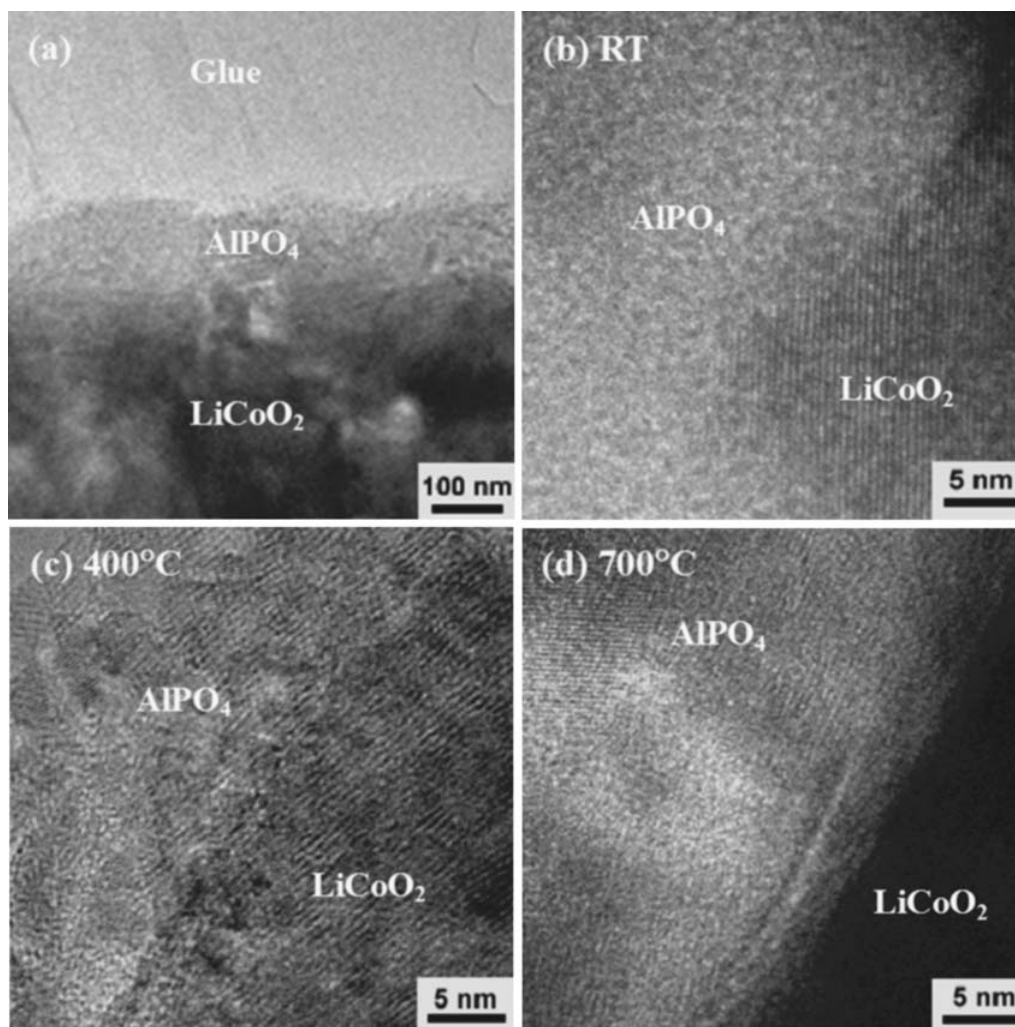
LiCoO_2 is the most popular among the possible cathode materials owing to the convenience and simplicity of preparation. This material can be easily synthesized using both solid-state and chemical approaches [4,5]. The Li_xCoO_2 exhibits excellent cyclability at room temperature for $1 > x > 0.5$. Therefore, the specific capacity of the material is limited to the range of 137 to 140 mAh/g, although the theoretical capacity of LiCoO_2 is 273 mAh/g [6]. On the other hand, Li_xCoO_2 is very expensive and highly toxic.

As for LiCoO_2 , coatings of carbon, various phosphates and oxides have been studied and significant improvements in capacity retention have been demonstrated. Carbon-coating can enhance the structural stability and electrical conductivity of LiCoO_2 [7], but LiCoO_2 may be reduced to CoO or Co_3O_4 by carbon [8]. Nanosized carbon coating has been deposited on LiCoO_2 by milling with sucrose followed by calcination in air [9]. The obtained composite cathode shows a higher capacity than the pristine LiCoO_2 , which is ascribed to the reduced charge transfer resistance and the faster Li-ion diffusion.

Apart from carbon coating, various MPO_4 ($\text{M} = \text{Al}, \text{Fe}, \text{SrH}$ and Ce) coatings on LiCoO_2 have attracted much interest. A co-precipitation method has been utilized to prepare FePO_4 -coated LiCoO_2 [10]. The FePO_4 coating improves the anti-overcharge and thermal stability as well as the structural stability. Kim et al. made an extensive study on the effect of the MPO_4 nanoparticle coatings on LiCoO_2 cathode material [11]. They found that the extent of the coating coverage is affected by the nanoparticle size and morphology despite the same coating concentration and annealing temperature. Smaller nanoparticles of AlPO_4 or FePO_4 with a size less than 20 nm fully encapsulate LiCoO_2 , whereas CePO_4 particles with a size larger than 150 nm or whisker-shaped SrHPO_4 only partially cover LiCoO_2 . Not surprisingly, the LiCoO_2 fully covered by AlPO_4 or FePO_4 exhibits the highest intercalation capacity of 230 mAh/g in a voltage range of 4.8 and 3 V at a rate of 0.1 C. The AlPO_4 -coated LiCoO_2 also shows the best capacity retention. Nevertheless, the CePO_4 - and SrHPO_4 -coated cathodes show better capacity retention than the FePO_4 -coated cathode at 90 °C, which is attributed to the continuous Fe metal ion dissolution at this temperature. The improvement in the electrochemical performance in the coated cathode is ascribed to the suppression of cobalt dissolution

and the non-uniform distribution of local strain by the coating layer. In a further investigation of AlPO_4 -coated LiCoO_2 , electrochemical properties of AlPO_4 -nanoparticle-coated LiCoO_2 at various cutoff-voltages were found to depend on the annealing temperature [12]. The AlPO_4 -coated cathodes exhibit excellent electrochemical performance with high cutoff voltages larger than 4.6 V when annealed at 600 and 700 °C, while such cathodes annealed at 400 °C show a lower capacity and poorer rate capability. However, the AlPO_4 -coated LiCoO_2 annealed at 400 °C showed optimal capacity retention [13]. Figure 2 shows typical TEM images of AlPO_4 -coated LiCoO_2 deposited at room temperature, 400 °C and 700 °C. A continuous layer of AlPO_4 with thickness of about 100 nm is coated on the surface of LiCoO_2 , as shown in Figure 2a. The coating layer deposited at room temperature is amorphous (Figure 2b). The coating deposited at 400 °C is composed of nanocrystals with size in the range of 3–5 nm (Figure 2c), and the coating deposited at 700 °C consists of ~20–30 nm sized nanocrystals (Figure 2d). The dependence of electrochemical properties on annealing temperature can be explained by the effect of temperature on the nanostructures of the coating layer and the interdiffusion at the interface between the coating layer and the LiCoO_2 cathode.

Figure 2. (a) Cross-sectional TEM images of AlPO_4 -coated LiCoO_2 . A ~100 nm thick AlPO_4 continuous layer is coated on the LiCoO_2 . High resolution images of the AlPO_4 -coated LiCoO_2 at (b) room temperature, (c) 400 °C, and (d) 700 °C. Adapted from [13]. Copyright 2006 The Electrochemical Society.



In addition to coatings of phosphates, surface modification of LiCoO_2 by coating various oxides such as ZrO_2 [14], Al_2O_3 [15], SnO_2 [16], MgO [17], ZnO [18] or $3\text{LaAlO}_3:\text{Al}_2\text{O}_3$ has been widely investigated. In the case of ZnO -coated LiCoO_2 , the ZnO coating reduces the cobalt dissolution and prevents the inorganic surface films such as LiF from covering the LiCoO_2 particles [18]. Moreover, the ZnO coating alleviates the cycle-life degradation caused by inappropriate conductive carbon. Based on the impedance spectra, the charge-transfer resistance of ZnO -coated LiCoO_2 is much smaller than the uncoated cathode, although the ZnO coating layer is more resistant than the LiCoO_2 surfaces. It can be concluded that surface modification with ZnO improves the high-voltage cycleability of the LiCoO_2 cathodes. In a similar manner, ZrO_2 coating protects the LiCoO_2 cathode surface and reduces the electrolyte decomposition at high voltages [19, 20]. The ZrO_2 -coated LiCoO_2 shows much better structural change behaviors than the bare LiCoO_2 , as evidenced by in situ XRD data. Cheng-Zhang Lu et al. have prepared LiCoO_2 coated with different wt% of $3\text{LaAlO}_3:\text{Al}_2\text{O}_3$ [21]. LaAlO_3 is used as the electrical conductor and amorphous Al_2O_3 help to collect PF_6^- , PF_5 and HF in the electrolyte. The $3\text{LaAlO}_3:\text{Al}_2\text{O}_3$ -coated LiCoO_2 with 1.0 wt% $3\text{LaAlO}_3:\text{Al}_2\text{O}_3$ exhibits the best electrochemical performance, showing a discharge capacity of 138 mAh/g after 182 cycles which is larger than that is retained by pristine LiCoO_2 after 38 cycles.

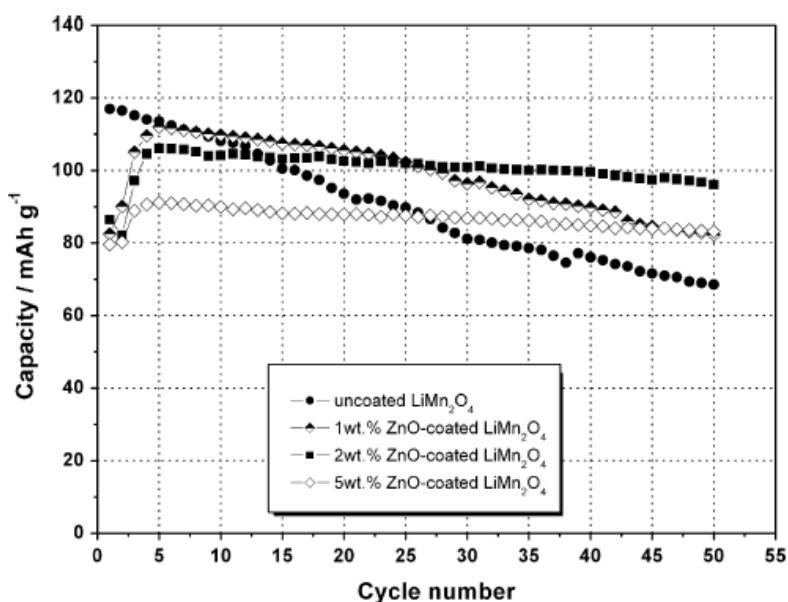
The battery cells discussed above all employ liquid organic electrolytes which are flammable and cause safety concerns. Replacing the liquid electrolyte with nonflammable solid electrolyte such as sulfide electrolyte is a solution to the safety problems, however, the energy densities and power densities of solid-state lithium batteries are relatively low for practical applications. One way to improve the rate capability of solid-state batteries is to add a buffer film with a thickness in nanometer scale between the electrode and electrolyte materials. A thin layer of $\text{Li}_4\text{Ti}_5\text{O}_{12}$ with thickness of a few nanometers was chosen to be coated on the LiCoO_2 cathode [22]. The $\text{Li}_4\text{Ti}_5\text{O}_{12}$ is also a Li intercalation material which ensures the electronic conduction, however, this material intercalates lithium ions at voltages lower than 1.5 V and thus does not act as intercalation material in the voltage range of LiCoO_2 . The power densities of the solid-state batteries with the thin $\text{Li}_4\text{Ti}_5\text{O}_{12}$ layer between the LiCoO_2 cathode and sulfide electrolyte are greatly increased and comparable to those of commercial lithium batteries, which is attributed to the suppression of the lithium-ion transfer. A mechano-thermal method has also been used to prepare $\text{Li}_4\text{Ti}_5\text{O}_{12}$ -coated LiCoO_2 particles [23]. The $\text{Li}_4\text{Ti}_5\text{O}_{12}$ coating suppresses the increase of the impedance and the dissolution of Co ions. In addition to $\text{Li}_4\text{Ti}_5\text{O}_{12}$ -coated LiCoO_2 , LiFePO_4 -coated LiCoO_2 has been fabricated via a impregnation method [24]. The LiFePO_4 coating suppresses the decomposition of the LiCoO_2 and protects the active sites as well.

LiMn_2O_4 is another popular cathode material for lithium-ion batteries. In comparison with LiCoO_2 , LiMn_2O_4 possesses essential advantages of less toxicity and having an abundant materials source. In principle, $\text{Li}_x\text{Mn}_2\text{O}_4$ permits the intercalation/extraction of lithium ions in the range of $0 < x < 2$ [25]. For intermediate values of x between 1 and 2 the material consists of two different phases—cubic in bulk and tetragonal at the surface. However, LiMn_2O_4 or substituted LiMn_2O_4 suffers from capacity fading especially at elevated temperatures. Coating of nanosized oxides on LiMn_2O_4 will help to improve its cycling performance. The electrochemical behavior of nanosized ZnO -coated LiMn_2O_4 was examined at 55 °C [26]. After 50 cycles at 55 °C, the coated LiMn_2O_4 shows capacity retention of 97%, much higher than the capacity retention (58%) of the bare cathode. ZnO coating collects HF

from the electrolyte and thus decreases the Mn dissolution in the electrolyte then subsequently reduces the interfacial resistance.

A sol-gel route has been used to coat nanosized ZnO on LiMn_2O_4 and ZnO coatings with different wt% are studied [27]. Figure 3 shows the capacity vs. cycle number profiles of ZnO-coated and uncoated LiMn_2O_4 when cycled between 3.4 and 4.3 V at 55 °C. The uncoated LiMn_2O_4 has higher initial discharge capacity but exhibits poor cycling stability, while ZnO (2 wt%)-coated LiMn_2O_4 shows the best cycling performance under a current rate of $C/2$. For the same reason, nanosized ZnO homogenously coated on the $\text{Li}_{1.05}\text{Al}_{0.1}\text{Mn}_{1.85}\text{O}_{3.95}\text{F}_{0.05}$ by a hydrothermal process was found to significantly improve cycling performance of the cathode at 55 °C [28]. The coated $\text{Li}_{1.05}\text{Al}_{0.1}\text{Mn}_{1.85}\text{O}_{3.95}\text{F}_{0.05}$ shows high capacity retention of 98.5% after 50 cycles.

Figure 3. Capacity vs. cycle number profiles of uncoated and ZnO-coated LiMn_2O_4 cycled at 55 °C, between 3.4 V and 4.3 V. Adapted from [27]. Copyright 2007 Elsevier.



Similarly, coating of amorphous ZrO_2 on LiMn_2O_4 can improve the high-temperature cycleability by picking up acidic species from electrolyte [29]. Moreover, the ZrO_2 -coated LiMn_2O_4 exhibits tremendously improved cycling stability at high rates up to 10C due to the following mechanisms. First, ZrO_2 can form a few stable phases with Li and thus amorphous ZrO_2 matrix possibly possesses high solubility of Li. Therefore, the ZrO_2 coating can act as a highly-Li conducting solid electrolyte interface which reduces the interfacial resistance. Second, the rigid oxide coating strongly bonds to LiMn_2O_4 which tolerates the lattice stress resulted from volume expansion during lithium intercalation. Lastly, ZrO_2 can collect HF from electrolyte to reduce Mn dissolution like ZnO does. The electrochemical behavior of ZrO_2 -coated stoichiometric LiMn_2O_4 and substituted $\text{Li}_{1.05}\text{M}_{0.05}\text{Mn}_{1.9}\text{O}_4$ ($\text{M} = \text{Al}, \text{Ni}$) cathodes were further compared with those of cathodes coated with Al_2O_3 and SiO_2 . ZrO_2 -coated $\text{Li}_{1.05}\text{M}_{0.05}\text{Mn}_{1.9}\text{O}_4$ ($\text{M} = \text{Al}, \text{Ni}$) shows the best cycling stability at 50 °C [30]. The ZrO_2 coating, deposited from colloidal suspensions, is porous network connected by ZrO_2 nanoparticles with dimensions less than 4 nm. This ZrO_2 network effectively scavenges HF from the electrolyte and

allows the access of the electrolyte to the cathode, and thus improves the high-temperature cycleability of the cathode.

$\text{Li}_4\text{Ti}_5\text{O}_{12}$ can also be coated on LiMn_2O_4 , because it has a high chemical diffusion coefficient ($10^{-6} \text{ cm}^2/\text{s}$) [31], the same spinel structure and zero-strain property as LiMn_2O_4 [32]. $\text{Li}_4\text{Ti}_5\text{O}_{12}$ -coated LiMn_2O_4 particles have been synthesized by a sol-gel method [33]. The LiMn_2O_4 particles are enwrapped by a $\text{Li}_4\text{Ti}_5\text{O}_{12}$ thin layer which is inactive to the electrolyte and does not expand during cycling. Hence, the decomposition of LiMn_2O_4 is hindered and the cycling stability is enhanced.

In addition to conventional lithium transition metal oxides such as LiCoO_2 , LiMn_2O_4 , and LiNiO_2 , their derivatives have drawn tremendous attention as the cathode materials in recent years. $\text{LiNi}_{0.8}\text{Co}_{0.2}\text{O}_2$ has both advantages of LiCoO_2 and LiNiO_2 , and shows better structural and thermal stability than both of them. However, the safety of $\text{LiNi}_{0.8}\text{Co}_{0.2}\text{O}_2$ needs to improve due to the poor thermal stability [34-36]. To solve this problem, $\text{LiNi}_{0.8}\text{Co}_{0.2}\text{O}_2$ is coated with Al_2O_3 [37] and $\text{Co}_3(\text{PO}_4)_2$ [38], respectively. The thin coating of Al_2O_3 (4-6 nm) separates the cathode with the liquid electrolyte, and thus reduces the side reactions. The $\text{Co}_3(\text{PO}_4)_2$ coating can also suppress the dissolution of Ni^{4+} . Moreover, the onset temperature of exothermic reactions is increased to 218 °C, which further improves the thermal stabilities. Compared to $\text{LiNi}_{0.8}\text{Co}_{0.2}\text{O}_2$, $\text{LiNi}_{1/3}\text{Co}_{1/3}\text{Mn}_{1/3}\text{O}_2$ shows better safety performance and higher capacity (~200 mAh/g), however, its cycling stability is not satisfactory at high voltage. A combination of co-precipitation method and spray drying process is utilized to prepare the ZrO_2 -coated $\text{LiNi}_{1/3}\text{Co}_{1/3}\text{Mn}_{1/3}\text{O}_2$ [39]. ZrO_2 scavenges the HF in the electrolyte and thus suppresses the increase of the cell resistance. Thus, the rate capacity and cycling stability are improved at a high cutoff voltage of 5 V.

2.2. Nanosized coatings on lithium phosphates

Lithium phosphate is presently the focus of much interest as the cathode for lithium-ion batteries, because it is inexpensive, abundantly available, environmentally friendly, thermally stable in the fully charged state and has a large theoretical capacity of 170 mAh/g. The results on the diffusion coefficient of LiFePO_4 are controversial, because there is no compositional variation and what is measured is the movement of the $\text{LiFePO}_4/\text{FePO}_4$ interface. A diffusion coefficient around 10^{-13} - $10^{-14} \text{ cm}^2/\text{s}$ over a whole range of composition was reported by Franger *et al.* for LiFePO_4 [40]. Another experimental work reported a value of $2 \times 10^{-14} \text{ cm}^2/\text{s}$ [41]. Most recently, a systematic study of LiFePO_4 with cyclic voltammetry (CV) has been presented [42]. In this study, the lithium diffusion coefficients were determined by CV to be 2.2×10^{-14} and $1.4 \times 10^{-14} \text{ cm}^2/\text{s}$ for charging and discharging LiFePO_4 electrodes in 1 M LiPF_6 ethylene carbonate/diethyl carbonate, respectively. There are essentially no electronically conducting species in pure LiFePO_4 . Therefore, the conductivity of the material is only 10^{-11} S/cm partially due to the motion of lithium ions [43]. Carbon containing precursors (e.g. carbonates, acetates and oxalates) are used to prepare LiFePO_4 so that some residual carbon will prevent the formation of ferric ions. The as-prepared samples show higher conductivities, in the range of 10^{-5} - 10^{-6} S/cm , however, it is not yet high enough for high power lithium batteries [44].

To increase the conductivity, the material could be doped as suggested by Chiang and coworkers [43]. However, doping may have deleterious impact if it occurs on the lithium sites. Conductive coatings deposited on the surface of LiFePO_4 are usually employed to solve the conductivity issue.

Most coatings are carbonaceous and deposited during the synthesis process. Among the carbon-coated LiMPO_4 ($M = \text{Fe, Mn, Co, Ni}$) composites, the LiFePO_4/C with surface carbon coating of 1.8 wt% achieves an electronic conductivity of 10^{-2} S/cm and shows the best electrochemical performance. Pioneering work on carbon coated LiFePO_4 was carried out by Ravet *et al.* [45,46]. Sucrose was used as one carbon source [46] and was added on the initial hydrothermal samples [47] or during pyrolysis [48]. Other methods include thermal decomposition of pyrene [49], hydrothermal decomposition of ascorbic acid [50], citric acid based sol-gel processing [51], modified mechanical activation (MA) of acetylene black [52], and a spray pyrolysis assisted with planetary ball-milling [53]. Even olive oil, soybean oil, or butter can be used as the carbon source [54]. Among these methods, samples synthesized by heat-treatments at 700 °C assisted with a hydrothermal method show an increased electrical conductivity [52]. The modified MA process helps to decrease the carbon content in the cathode, and thus increase the energy density. The electrode prepared via a spray pyrolysis assisted with the planetary ball-milling shows a nearly constant discharge capacity of 114 mAh/g over 100 cycles at the 5 C rate, demonstrating excellent rate capacity and cycling stability.

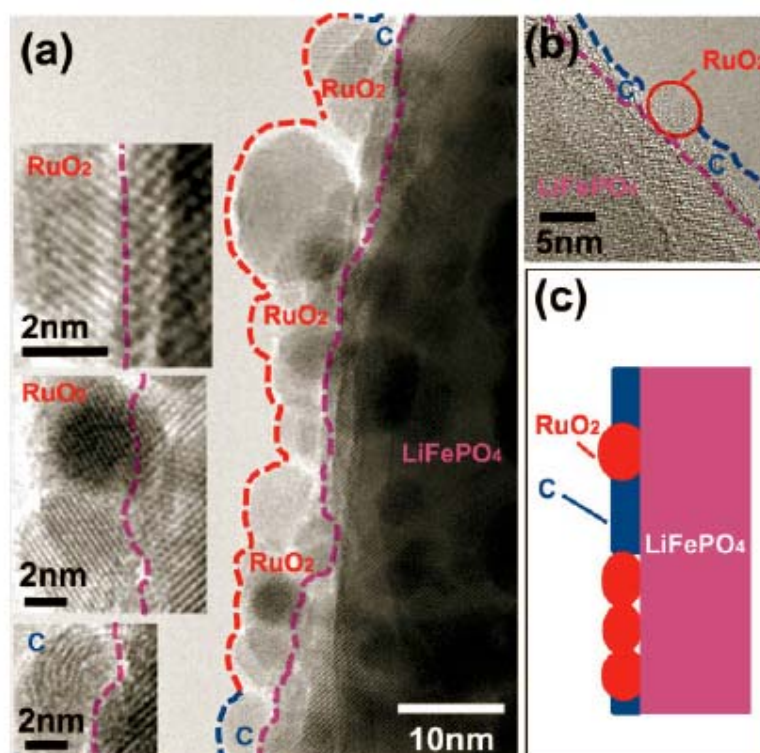
It should be noted that the electrochemical properties of LiFePO_4 are influenced by the quality of carbon coatings. Wilcox *et al.* found that the conductivity and rate behavior of LiFePO_4 are strongly affected by carbon structural factors such as sp^2/sp^3 and disordered/grapheme (D/G), as determined by Raman spectroscopy, and H/C ratios determined from elemental analysis [55]. The structure of carbon can be controlled by the use of additives during LiFePO_4 synthesis. LiFePO_4 coated with the more graphitic carbon has higher conductivity and shows better electrochemical performance. Another factor that influences the electrochemical performance of LiFePO_4/C composites is the porosity. Gaberscek *et al.* prepared micro-sized porous LiFePO_4/C particles with different morphology by using different techniques such as solid-state or sol-gel methods [56]. The composite porosity is influenced by synthesis and synthesis parameters. The composites prepared at a relatively high heating rate ($>5\text{K/min}$) have interconnected pores and show the best electrochemical performance, e.g., more than 140 mAh/g at C/2 rate during continuous cycling.

In addition to carbon coating, metal coating such as silver [57] and oxide coating such as zinc oxide [58] have been successfully used to increase the conductivity as well. ZnO-coated LiFePO_4 shows better cycling performance than bare LiFePO_4 , because ZnO coatings improve the chemical stability of LiFePO_4 by hindering the iron dissolution. Another type of coating is conductive inorganic layer such as metallic Fe_2P , as investigated by Rho *et al.* [59]. In their study, mixture of Fe_2P and FeP were deposited on the surface of the LiFePO_4 along with carbon and the by-product Li_3PO_4 by surface reduction reactions. Fe_2P is coated directly on the LiFePO_4 , while carbon and Li_3PO_4 sit on the outer surface of the crystallites. Such surface layer structure facilitates significantly improved rate capabilities and superior cycleability: a high capacity of 105 mAh/g is achieved at a very high rate of 14.8C. Recently Wang and Su's group have designed a LiFePO_4 spherical structure coated by a π -bond character planar polymer - polyacene (PAS) - by pyrolysis of the phenol-formaldehyde resin [60]. The conductivity of LiFePO_4 -PAS structure is drastically increased to 10 S/cm. High capacities and excellent cycling performance are achieved for the LiFePO_4 -PAS structure in a wide temperature range of -20 to 60 °C. In another study presented by Goodenough's group, conductive polymer polypyrrole (PPy) was bonded to LiFePO_4 particles by a carbon coat and was found to significantly improve the capacity and rate capability of LiFePO_4 [61]. For example, at a high rate of 10C, the

C-LiFePO₄/PPy containing 16 wt% PPy shows a high capacity and steady cycling performance. C-LiFePO₄/PPy composites can also be synthesized by electrochemical deposition and simultaneous chemical polymerization, in which PPy substitutes the inactive carbon and thus improves the electrochemical performance [62].

In a similar manner, electronically conducting RuO₂ was used as an oxidic nanoscale interconnect for carbon containing porous LiFePO₄ to improve electrode performance [63]. RuO₂ with a particle size of about 5 nm was deposited on the carbon-LiFePO₄ with an average pore size of 50 nm by using cryogenic decomposition of RuO₄ at low temperature. The resulting C-LiFePO₄/RuO₂ composite maintains the morphology and structure of the original C-LiFePO₄, as revealed by high-resolution TEM images in Figure 4. Nanosized RuO₂ as an oxide adheres well with oxides such as LiFePO₄, while simultaneously assures good contact with carbon. Hence, RuO₂ repairs incomplete carbon network in porous LiFePO₄ and thus improves the kinetics and rate capability of the composite. It is found that the original C-LiFePO₄ electrode shows decent performance at low current rates but the performance deteriorates at high current rates. The C-LiFePO₄/RuO₂ shows improved electrochemical behavior at high rates.

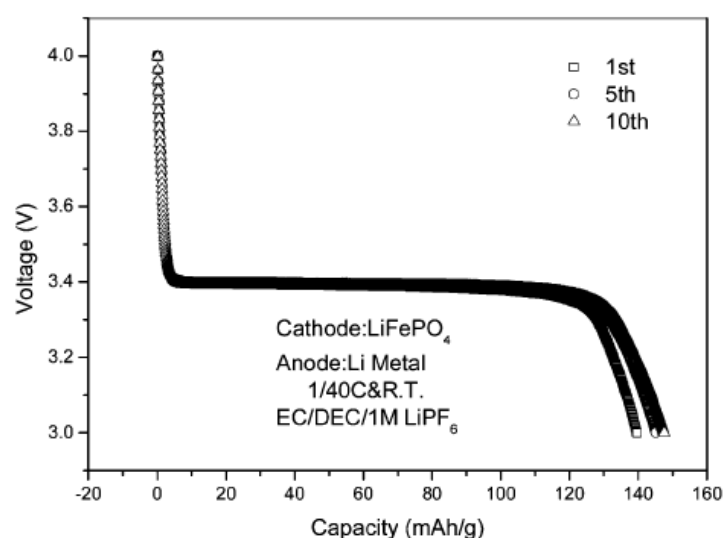
Figure 4. (a and b) High resolution TEM images of C-LiFePO₄ after RuO₂ coating. (c) Schematic of the repair of the electronically conducting network of carbon on porous LiFePO₄ by nanosized RuO₂. Adapted from [63]. Copyright 2007 Wiley-VCH.



The problems of low electronic conductivity and slow diffusion of lithium ions in LiFePO₄ can be further alleviated by modifying with conductive species and by minimizing particle size simultaneously, for example, a nanocomposite of LiFePO₄ with a carbon xerogel could be formed from a resorcinol-formaldehyde precursor. This nanocomposite achieves 90% theoretical capacity at C/2 with

very good stability at room temperature [64]. Such excellent electrochemical performance is attributed to modification with carbon and control of particle size to nanometer scale. Both factors are of essential importance. The nanosized LiFePO_4 /carbon composites with dimensions in the range of 20–30 nm could also be prepared by using citric acid as a complexing agent and a carbon source, which suppresses the growth of LiFePO_4 particles and enhances the conductivity of the composites [65]. The carbon-coated LiFePO_4 sintered at 850 °C demonstrates the highest conductivity of 2.46×10^{-3} S/cm and best electrochemical properties, as shown in Figure 5. The discharge profile is flat over a wide voltage range, due to the two-phase redox reaction via a first-order transition between FePO_4 and LiFePO_4 [66]. A discharge capacity of 148 mAh/g is achieved for this cathode material. A slight increase in capacity is observed after a few cycles, showing good cycleability.

Figure 5. Discharge curves of LiFePO_4 /carbon sintered at 850 °C for 2 hours. Adapted from [65]. Copyright 2004 Royal Society of Chemistry.



3. Nanostructured Composites as Cathode Materials

Most cathode materials with interesting thermodynamic properties are typically ceramic materials with low electronic conductivity ranging from 10^{-3} S/cm for LiCoO_2 [67] down to 10^{-9} S/cm for LiFePO_4 [43]. To improve the electrochemical kinetics, the cathode materials need to be embedded within an electronically-conducting network, e.g., some thin coating of conductive material. The coatings must be thin enough, within nanoscale so that ions can penetrate through them without appreciable polarization. Furthermore, the internal electrical field generated by electrons may enhance the ionic motions [68]. Such surface modifications alleviate the problem of low electronic conductivity, at the same time, reducing the size of active material would shorten the diffusion length for lithium. The realization of such nanostructured composites consisting of cathode materials and conductive additives makes it possible to utilize theoretical capacities at intermediate or even higher rates.

3.1. Nanostructured carbon-oxide composites

One of the commonly studied carbon-based composites is carbon-vanadium oxide composite. Vanadium oxide is a typical intercalation compound as a result of its layered structure. For Li-ion intercalation applications, vanadium oxide offers the essential advantages of low cost, abundant source, easy synthesis, and high energy densities. Orthorhombic crystalline V_2O_5 consists of layers of VO_5 square pyramids that share edges and corners [69,25]. The reversible electrochemical lithium intercalation into V_2O_5 at room temperature was first reported by Whittingham in 1975 [70]. Carbon-coated V_2O_5 nanoparticles can be synthesized via burning off carbon-coated V_2O_3 nanoparticles around 400 °C in air [71]. The thickness and weight percentage of carbon can be manipulated by varying the conditions of the burning process. The optimal carbon content is found to be 2-3% by weight. Because of the carbon coating, these C- V_2O_5 nanoparticles have good interparticle electrical contact, and do not have the usual drawbacks of nanoparticles such as poor active mass integrity and high surface reactivity. Therefore, carbon-coated V_2O_5 nanoparticles are found to have higher capacity, better rate capability and cycleability than V_2O_5 microparticles or nanoparticles. The Li intercalation capacity of C- V_2O_5 nanoparticles reaches 290 mAh/g at high rates.

Higher capacities can be achieved with vanadium oxide/carbon nanotube nanocomposites. Dunn's group incorporated V_2O_5 aerogels into single-wall carbon nanotubes using a sol-gel method [72]. The carbon nanotubes and V_2O_5 nanoribbons in the aerogel have similar morphology and dimensional scale, and thus have intimate contact with each other in the nanoscale. Moreover, the porous structure of carbon nanotubes and V_2O_5 aerogel permits electrolyte access throughout the composite material. As a result, such nanocomposite electrode shows high capacities exceeding 400 mAh/g at high rates. Akira Kuwahara *et al.* have prepared V_2O_5 -C composites by drying the precursor which contains V_2O_5 sol, carbon and a surfactant [73]. The authors claim that short lithium diffusion distance (< 13 nm) and high electric conductivity (> 3.4 S/cm) are both required to attain good electrochemical performance at a high discharge rate (30 A/g).

Apart from vanadium oxides, some nanostructured lithium vanadium oxides have also been reported to form nanocomposite with carbon which exhibits excellent electrochemical characteristics. It was reported that mixing the precursor of $Li_{1+\alpha}V_3O_8$ with a suspension of carbon black resulted in nanocomposites of $Li_{1+\alpha+x}V_3O_8/\beta-Li_{1/3}V_2O_5/C$ [74]. $\beta-Li_{1/3}V_2O_5$ was a by-product formed when the initial $Li_{1+\alpha}V_3O_8$ was reduced by carbon. Here carbon particles play critical roles as a reducing agent, a growth-limiting agent to restrict the electroactive material within the nanoscale, and as an electronically conducting agent. The $Li_{1+\alpha+x}V_3O_8/\beta-Li_{1/3}V_2O_5/C$ nanocomposite shows significantly better electrochemical performance in comparison with the standard $Li_{1+\alpha}V_3O_8$.

In addition to traditional nanostructured layered materials that intercalate guest species between the interlayers, there are other inorganic compounds demonstrating high lithium storage capacity by electrochemically reacting with lithium ions. For example, the lithium intercalation of nanostructured manganese oxide involves formation/decomposition of lithium oxide, which is facilitated by formation of metallic manganese. Similar to other transition metal oxides, MnO_2 also has the problem of poor electric conductivity. Carbonaceous material can be added to MnO_2 to improve the electronic transport. MnO_2 -CNT hybrid coaxial nanotubes have been fabricated from porous alumina template by vacuum infiltration assisted with chemical vapor deposition [75]. The MnO_2 -CNT composites exhibit a

shell-core structure, in which the CNTs improve the electric conductivity considerably, supply a buffering zone, and contribute to the reversible capacity. Such nanocomposite electrode delivers a capacity higher than the unsupported MnO_2 nanotubes by one order of magnitude. Similar to carbon black, acetylene black was also used to prompt the reduction of potassium permanganate, yielding amorphous manganese oxide/carbon composites [76]. The as-prepared composite delivers a high capacity of 231 mAh/g at a current density of 40 mA/g, showing good electrochemical performance at high rates.

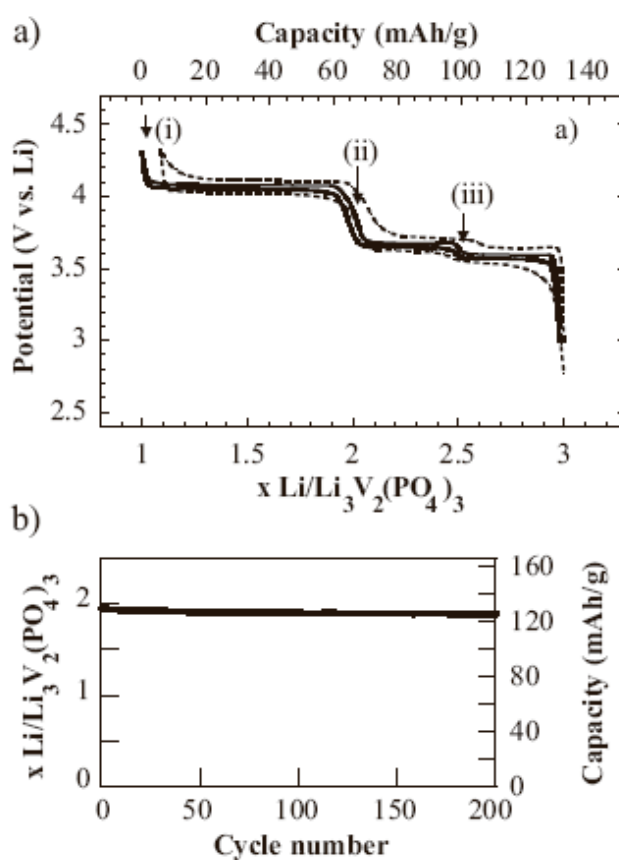
The energy density of MnO_2/C nanocomposite can be further increased by optimization of the synthesis conditions. The MnO_2/C nanocomposite can be obtained via a sonochemical synthesis method using acetylene black and sodium permanganate. Synthesis conditions such as the reaction temperature and specific surface area of the carbon have been optimized to achieve the best electrochemical performance of the nanocomposite [77]. The active material content increases by increasing the reaction temperature. It is interesting to note that the capacity increases with the increasing amount of active material then decreases, because the excessive formation of active material increases the electrochemically effective volume, leading to capacity drop. On the other hand, using carbon with higher surface area results in higher capacity; the highest capacities are 126 and 99.9 mAh/g at current densities of 1 and 10 A/g, respectively.

A number of lithium phosphates/carbon composites have also been studied as cathode materials for lithium batteries, including those of general formula LiMPO_4 ($\text{M} = \text{Fe}, \text{Mn}, \text{Co}, \text{Ni}$) [78] and $\text{Li}_3\text{V}_2(\text{PO}_4)_3$ [79]. Among these lithium transition metal phosphates with an olivine-type structure, LiFePO_4 attracts considerable interest since 1997 [66] due to its low cost, environmental compatibility, thermal stability and relatively high theoretical capacity (170 mAh/g) [52,80,81]. Forming composite with carbonaceous material can reduce the resistance and increase the rate capacity of the electrodes. The $\text{LiFePO}_4\text{-C}$ nanoparticles have been prepared by solid-state reaction [82]. It is found that the discharge capacities change with different carbon source. Bo Jin *et al.* [83] have synthesized the LiFePO_4 -multiwalled CNT by a combination of hydrothermal method, ball-milling and heating. The size of particles is influenced by the multiwalled CNTs. And the electronic conductivity is further improved up to $1.08 \times 10^{-1} \text{ S/cm}$.

Compared to LiFePO_4 , that attracts a lot of attention, $\text{Li}_3\text{V}_2(\text{PO}_4)_3$ is relatively unexplored. $\text{Li}_3\text{V}_2(\text{PO}_4)_3$ has a high operating voltage of 4.0 V and a theoretical lithium storage capacity of 197 mAh/g [79,84-88]. However, this material also suffers from low electronic conductivity similar to LiFePO_4 . To solve this issue, $\text{Li}_3\text{V}_2(\text{PO}_4)_3$ crystallites were wrapped within a conductive carbon network to form a nanocomposite which delivers almost full capacity at high rates [79]. The potential curves in Figure 6(a) reveal that two lithium ions per formula unit are completely extracted in three steps to give a theoretical capacity (100%) of 132 mAh/g at a rate of $C/5$. 95% theoretical capacity is still achieved at a high rate of $5C$. The flat plateaus in the curve correspond to $\text{Li}_x\text{V}_2(\text{PO}_4)_3$, where $x = 2.5$ (i); 2.0 (ii); and 1.0 (iii). Such a sequence of phase transitions between two single phases shows the very low degree of polarization in the discharge curve owing to the facile ion and electron transport. Excellent cycling stability is also demonstrated by this material, as shown in Figure 6(b). When cycled between 3.0 V and 4.8 V, the $\text{Li}_3\text{V}_2(\text{PO}_4)_3/\text{C}$ composite delivers a specific energy density of 2,330 mWh/cm³ comparable to LiCoO_2 (2,750 mWh/cm³) or LiFePO_4 (2065 mWh/cm³). Nanocarbon-coated $\text{Li}_3\text{V}_2(\text{PO}_4)_3$ prepared via a sol-gel process has also been reported [89]. Another

promising substitute for LiCoO_2 is $\text{Li}[\text{Ni}_{1/3}\text{Mn}_{1/3}\text{Co}_{1/3}]\text{O}_2$ due to its thermal stability [90], low cost, and low toxicity [91]. However, the electrical conductivity of $\text{Li}[\text{Ni}_{1/3}\text{Mn}_{1/3}\text{Co}_{1/3}]\text{O}_2$ is not as satisfactory as that of LiCoO_2 [92]. Carbon coating on the $\text{Li}[\text{Ni}_{1/3}\text{Mn}_{1/3}\text{Co}_{1/3}]\text{O}_2$ is proved to improve the electrical conductivity and thus enhance the high rate capacity [64]. Citric acid [91] and super P carbon black [92] have been used as carbon sources to prepare the C-coated $\text{Li}[\text{Ni}_{1/3}\text{Mn}_{1/3}\text{Co}_{1/3}]\text{O}_2$. The resulted nanocomposite electrodes show better cycling performance, rate capability and thermal stability.

Figure 6. (a) Voltage-composition plot for $\text{C}/\text{Li}_3\text{V}_2(\text{PO}_4)_3$ composites at rates of C/5 (solid line) and 5C (dotted line) in the potential window 3.0 – 4.3 V; single phase compositions are indicated: $x = 2.5$ (i); 2.0 (ii); and 1.0 (iii). (b) Cycling stability at a rate of 1C. Adapted from [79]. Copyright 2002 Wiley-VCH.



3.2. Nanostructured polymer-oxide composites

Over the past two decades much interest has been placed on the conductive polymer/transition metal oxide nanocomposite. The hybrid material consists of conductive organic polymers (e.g., polyacetylene, polyaniline and polypyrrole (PPy), pyridinesulfonic acid (PSA)) interleaved between the layers of an oxide lattice such as V_2O_5 . Both oxide and polymer are electrochemically active and this feature makes the polymer/oxide nanocomposite very attractive as the cathode material for lithium batteries. A PSA-PPy- V_2O_5 composite has been prepared via a chemical polymerization process [93]. The addition of PSA increases the spacing between the oxides, resulting in a more homogenous hybrid material with better electrochemical characteristics. The Layer-by-Layer (LbL) technique, based on

physical adsorption of oppositely charged layers, has been widely used to prepare V_2O_5 nanocomposites alternating with polymer layers. One popular example is V_2O_5 /polyaniline nanocomposite film fabricated by the LbL technique and the intimate contact between the oxide and polymer within nanoscale results in an improved intercalation capacity [94]. Later, V_2O_5 nanocomposite alternating with blends of chitosan and poly(ethylene oxide) (PEO) was prepared using the LbL technique and investigated the charge storage capability in such nanoarchitectures [95]. A small amount of chitosan (1%) is added to blend with PEO because the adsorption of alternate layers of PEO and V_2O_5 is not efficient. The V_2O_5 /blend shows higher capacity and intercalates 1.77 moles of lithium per mole of V_2O_5 . The enhanced electrochemical performance of V_2O_5 /blend in comparison with V_2O_5 /chitosan is due to a larger number of electrochemically active sites and faster lithium diffusion within the host material. At 20 mV/s, the charges injected were 3.29 mC/cm² and 8.02 mC/cm² for V_2O_5 /chitosan and V_2O_5 /blend, respectively.

In a more recent report, polyaniline homogeneously distributed into V_2O_5 /polyaniline nanocomposite was found to stabilize the capacity [96]. In this study, a reverse micelle method was used to prepare V_2O_5 /polyaniline nanofibers which exhibit improved cycling performance compared to the V_2O_5 nanofibers [96]. The V_2O_5 /polyaniline nanofibers containing 30 mol% polyaniline delivers a steady capacity of about 300 mAh/g without morphology change over 10 cycles, whereas the V_2O_5 nanofibers do not retain the morphology after cycling. Some V_2O_5 /polymer nanocomposite shows lower storage capacity but better cycling stability compared to pure nanostructured V_2O_5 [97]. As reported by Reddy *et al.*, $PVP_xV_2O_5$ ($x = 0.5, 1$) nanobelts synthesized by a hydrothermal method exhibit lower capacity but better cycleability compared with V_2O_5 nanobelts. The authors studied the interaction between the oxide and polymer with Fourier transformation infrared spectroscopy (FTIR) and found that the hydrogen atoms in PVP are hydrogen-bonded with the oxygen atoms of the V=O bonds of V_2O_5 nanobelts, which effectively shields the electrostatic interaction between V_2O_5 interlayer and lithium ions. As discussed above, polymers can be intercalated between the interlayers of V_2O_5 , on the other hand, V_2O_5 can be interleaved within a block polymer matrix as well [98]. Mayes and coworkers used a sol-gel method to prepare continuous and amorphous V_2O_5 phase within the poly(oligooxyethylene methacrylate) (POEM) domains of a poly(oligooxyethylene methacrylate)-block-poly(butyl methacrylate) (POEM-*b*-PBMA) copolymer (70 wt% POEM) up to weight ratios of 34% V_2O_5 [98]. The resulted nanocomposite film is flexible and semi-transparent and the redox activity of V_2O_5 is preserved in such nanocomposite.

Cathode materials other than V_2O_5 can form nanocomposites with conductive polymer as well. Poly(ethylene oxide) (PEO) was used as an electroactive polymeric binder to mix with carbon containing $Li_{1.1}V_3O_8$ [99]. The resulted composite electrode shows a capacity of 270 mAh/g at a rate of C/5, higher than the capacity (180 mAh/g at C/5 rate) of the standard electrode without PEO. Such improved electrode performance is attributed to the more efficient charge-carrier collection within the composite electrode. Among all known cathode materials, elemental sulfur is the cheapest and has the highest theoretical capacity density of 1,672 mAh/g, assuming a complete reaction to yield Li_2S [100]. However, Li/S cells suffer from low utilization of active material, because electrochemical reaction with the interior active materials is hindered by the insulated reaction products covering the sulfur particles. Moreover, the dissolved polysulfides transfer onto the surface of the Li anode, causing lithium corrosion and poor rechargeability of Li/S cells. To overcome these two problems,

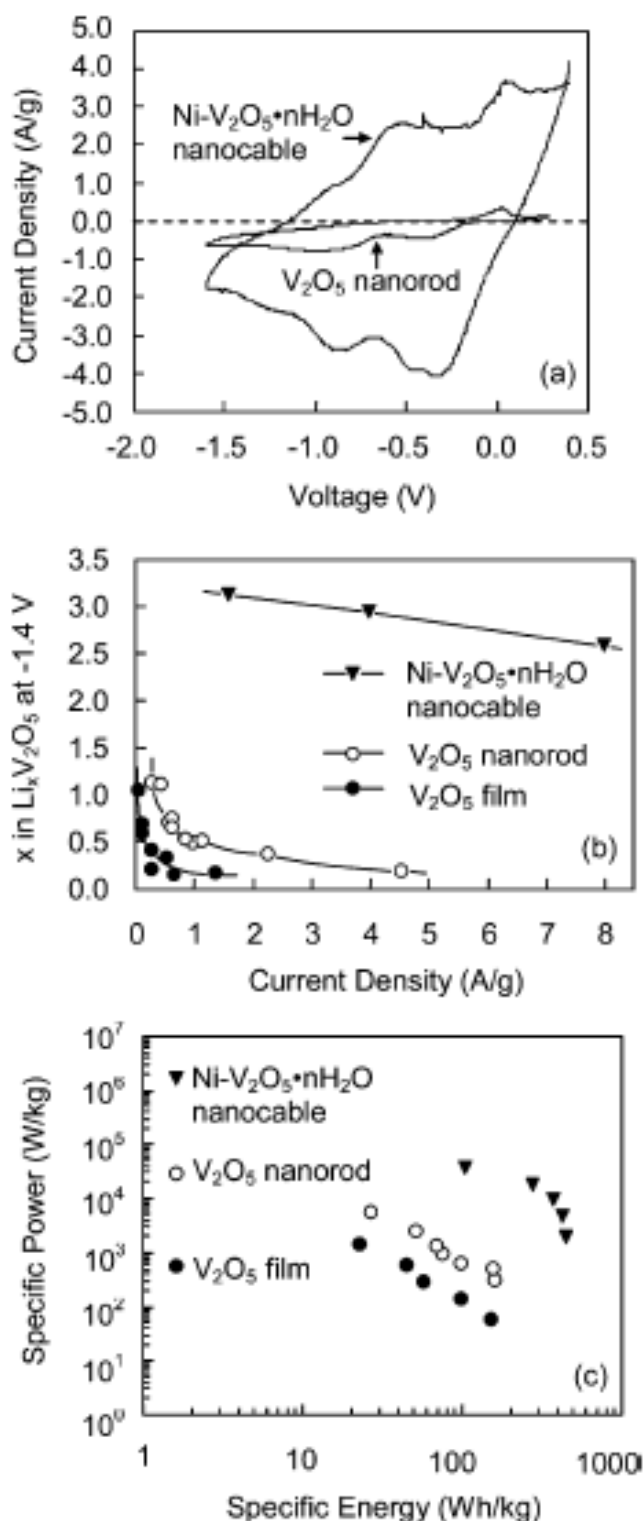
nanodispersed composites with sulfur embedded in a conductive polymer matrix were designed and prepared by heating the mixture of polyacrylonitrile (PAN) and sublimed sulfur [101,102]. The composite also show excellent cycling life due to the suppressed dissolution of polysulfides into the electrolyte and thus demonstrates a great potential as cathode material for lithium batteries. Conductive polymers themselves can act as cathode material, however, they suffer from low capacities and display sloping charge-discharge curves. For example, polypyrrole (PPy) is one of the most popular conductive polymers and has a specific energy ranging from 80 to 390Wh/kg [100]. To improve its capacity, a $\text{Fe}^{\text{III}}/\text{Fe}^{\text{II}}$ redox couple is physically or chemically attached to the PPy polymer backbone [103]. The examination of the PPy/ LiFePO_4 composite electrode shows that the composite has higher specific capacity and rate capability.

3.3. Nanostructured metal-oxide composites and other nanocomposites

The third most popular composite cathode is metal based cathode material, exemplified by the $\text{Ni-V}_2\text{O}_5 \cdot n\text{H}_2\text{O}$ core-shell structure. A two-step electrodeposition method has been used to prepare $\text{Ni-V}_2\text{O}_5 \cdot n\text{H}_2\text{O}$ core-shell nanocable arrays [104]. Ni nanorod arrays were first grown by the template-based electrochemical deposition. In the second step, the hydrated vanadium pentoxide shell was deposited onto the surface of nickel nanorods through sol electrophoretic deposition. Figure 7 compares the electrochemical performance of $\text{Ni-V}_2\text{O}_5 \cdot n\text{H}_2\text{O}$ nanocable arrays, single-crystal V_2O_5 nanorod arrays and sol-gel derived V_2O_5 films. Obviously $\text{Ni-V}_2\text{O}_5 \cdot n\text{H}_2\text{O}$ nanocable arrays demonstrate remarkably improved capacity and rate capability in comparison with the other two. The intercalation capacities of both nanorod arrays and sol-gel films decrease rapidly as the current density increases, while nanocable arrays are able to retain the high capacity at high current density (discharge rate), indicating the excellent high-rate performance of nanocable arrays. As shown in Figure 7c, $\text{Ni-V}_2\text{O}_5 \cdot n\text{H}_2\text{O}$ nanocable array has significantly higher energy density and power density than those of the nanorod array and sol-gel film by at least one order of magnitude, which is ascribed to the enhanced surface area and the reduced internal resistance.

Accordingly, Wang *et al.* synthesized $\text{Ag-Ag}_{0.08}\text{V}_2\text{O}_5 \cdot n\text{H}_2\text{O}$ composite films by dispersing silver nanowires into $\text{V}_2\text{O}_5 \cdot n\text{H}_2\text{O}$ matrix [105]. The composite film is found to deliver twice the capacity of the $\text{V}_2\text{O}_5 \cdot n\text{H}_2\text{O}$ xerogel film, due to further amorphization of $\text{V}_2\text{O}_5 \cdot n\text{H}_2\text{O}$, the increased porosity and the enhanced electronic conductivity. In a similar concept, $\text{LiCoO}_2\text{-Ag}$ composites have been fabricated [106]. It is suggested that Ag just enters the spacing between layers rather than substitutes the Li or Co. $\text{LiCoO}_2\text{-Ag}$ multilayer film was fabricated by magnetron sputtering and showed enhanced rate capability in comparison with LiCoO_2 film of the same thickness [107]. Thickness of Ag layer is restricted within nanoscale and the rate capability of the multilayer film improves with the increased thickness of Ag layer as a result of the enhanced electronic conductivity. A citrate–nitrate combustion synthesis technique has been utilized to prepare a $\text{LiCoO}_2\text{-Ag}$ composite material [106]. Ag slows the decomposition in the combustion process and enhances the electrical conductivity. In the study of Rui Guo *et al.*, a thermal decomposition method has been used to disperse Ag on the surface of $\text{Li}[\text{Ni}_{1/3}\text{Co}_{1/3}\text{Mn}_{1/3}]\text{O}_2$ [108]. The addition of Ag not only improves the electrical conductivity, but also protects the SEI film. Ag can also improve the cycling stability and high-rate discharge capacity of the LiMn_2O_4 electrode when dispersed on the surface using the thermal decomposition method [109].

Figure 7. (a) Cyclic voltammograms of Ni-V₂O₅·nH₂O nanocable array and V₂O₅ nanorod array using a scan rate of 10 mV/s. (b) Relationship between current density and Li intercalation capacity of Ni-V₂O₅·nH₂O nanocable array, V₂O₅ nanorod array and sol-gel film from chronopotentiometric measurements. (c) Ragone plot for Ni-V₂O₅·nH₂O nanocable array, V₂O₅ nanorod array and sol-gel film. Adapted from [104]. Copyright 2005 American Chemical Society.



More recently, oxide/metal/polymer composites have been obtained showing very good electrochemical performance. One example is freestanding $V_2O_5/Pt/PVA$ multilayer films with the thicknesses of the V_2O_5 , Pt, and PVA at 22, 57, and 704 nm [110]. Other types of composite structures include oxide/oxide composite such as $LiFePO_4-LiCoO_2$ and $ZnO-LiFePO_4$ composites. A double-layer cathode composed of a $LiCoO_2$ main layer with a $LiFePO_4$ sublayer on top of Al current collector which shows better tolerance against overcharging than other electrodes including ($LiCoO_2-LiFePO_4$ mixture)/Al single layer and $LiFePO_4/LiCoO_2/Al$ double layer [111]. The enhanced electrochemical performance is attributed to a large increase in the ohmic resistance of the delithiated Li_xFePO_4 layer which shuts the charging current down during overcharging without shut-down of the separator. The third type of composite structure is polymer/carbon nanocomposite, such as polyaniline (PANI)/multiwalled carbon nanotube (CNT) composite synthesized via in situ chemical polymerization. This nanocomposite is utilized as a cathode material in a lithium metal-polymer cell assembled with ionic liquid electrolyte [112]. Such a cell demonstrates a maximum discharge capacity of 139 mAh/g with good cycleability and shows decent high rate performance (111 mAh/g at the 2.0C rate).

4. Nanostructured Composite as Anode Materials

4.1. Nanostructured silicon-carbon composites

Silicon is considered one of the best substitutes for carbon anodes, owing to its high theoretical capacity (4,200 mAh/g), low cost and abundant source [113-115]. However, bulk Si electrodes show a 400% volume variation during Li-ion insertion/extraction processes [116], which will damage the structure of electrodes and cause huge capacity loss. Dispersing Si uniformly in a host matrix proves to be an effective method to solve this problem. Carbon is not only a conductive additive, but also supplies a ductile host matrix for dispersing Si nanoparticles [117]. In addition, carbon contributes to the capacity since Li can be intercalated into carbon as well [118]. As a result, the Si-C composite shows higher capacity than bare carbonaceous materials and better cycling stability than unsupported Si electrodes [119]. A composite material composed of nano-Si dispersed in carbon was reported as early as in 1995 [120]. Jie Shu *et al.* have synthesized a cage-like CNTs/Si composite using a chemical vapor deposition method [121]. In this structure, the Si particles are wrapped by a cage formed from tortile carbon nanotubes (CNTs). The CNTs improve the conductivity and are covered by a solid electrolyte interphase (SEI) film which improves the cycling stability of the electrode. The Si-C composite can also be prepared by dispersing nanocrystalline Si into the carbon aerogel [119]. This type of Si-C composite delivers a discharge capacity of about 2,000 mAh/g at the C/10 rate in the first cycle and a nearly constant capacity of 1,450 mAh/g after 50 cycles.

Other than the relatively simple Si-C composites that have demonstrated their capability in improving the performance of anodes as discussed above, there are other composites with complex structures which can be used to increase the capacity and enhance the cycling stability of anodes as well. A ball milling method has been employed to prepare a composite anode material of silicon/graphite/CNTs [118]. This preparation method of ball milling generates structural defects in multi-walled carbon nanotubes (MWNTs) and leads to MWNTs with shorter length. However, it is

interesting to note that the structural defects benefit the Li-ion storage and the shorter length of MWNTs facilitates the Li-ion diffusion [122]. MWNTs are added into the silicon/graphite composite due to their remarkable resiliency [123,124] and good electric conductivity [125]. Moreover, the network of MWNTs can enwrap the flaked graphite particles tightly, which further reduces the effect of the volume variation during Li-ion insertion/extraction process. Other composites with complex structures include a carbon-coated nano-Si dispersed oxide/graphite composite material prepared by Heon-Young Lee *et al.* [126]. In this structure, the graphite and inactive oxide are mainly used as the elastic matrix; the carbon-coating suppresses the side reactions between the electrolyte and the surface graphite particles and enhances the electrical contact of the Si and the graphite.

4.2. Nanostructured tin-carbon composites

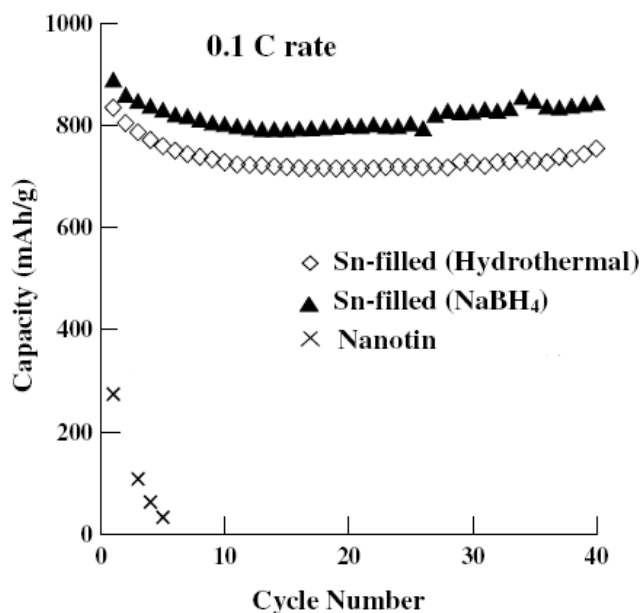
Apart from the Si-C composites, the Sn-C composites also show excellent electrochemical performances as anode materials. Sn has a lower active voltage (0.3 V) than that of Si (>0.5 V) [127] and has a very large theoretical capacity (994 mAh/g) as one mole of Sn can store 4.4 moles of Li [128]. However, the drastic volume variation (>300%) during Li-ion insertion/extraction process still limits its practical applications [129].

The cycling stability of Sn can be improved by dispersing Sn into a carbon matrix which functions as a buffer. Bingkun Guo *et al.* have recently prepared the Sn-C composite by embedding Sn nanoparticles into the mesopores of hard carbon spherules [130]. The initial coulombic efficiency (charge capacity divided by discharge capacity) is increased remarkably due to the SEI film induced by nano-Sn. In the study of Gaelle Derrien *et al.*, Sn nanoparticles are dispersed in a carbon matrix by infiltrating a tin precursor into an organic gel followed by calcinations [128]. Volume contraction occurs in the calcinations process and creates open space in the structure, which helps to alleviate the effect of volume change during Li-ion insertion/extraction process.

Carbon nanotube (CNT) has a capacity of more than 1,400 mAh/g as the anode material, but its practical application is limited due to the poor cycling stability [131-135]. T. Prem Kumar *et al.* have reported their synthesis of tin-filled carbon nanotubes via a hydrothermal reduction process and a NaBH₄-reduction process [135]. Figure 8 shows the cycling performances of nanotin and tin-filled carbon nanotubes. The overall capacity and the cycling stability of tin-filled carbon nanotubes are improved compared to unsupported Sn and MWNT. Such nanocomposite electrode exhibits a capacity of 1,082 mAh/g for the hydrothermally reduced product and 1,585 mAh/g for the NaBH₄-reduced product at the 0.1C rate. The capacities of the two products retain 754 and 844 mAh/g over 40 cycles, respectively.

Coating Sn with carbon is another method to prepare the Sn-C composite. Carbon-coated Sn nanoparticles have been synthesized via a hydrothermal method [136], or by mechanical mixing and heating the precursor subsequently [137]. MgO is added in the precursor to hinder the agglomeration of molten Sn and to provide free space for Sn after the MgO is dissolved.

Figure 8. Cycling performances of nanotin and tin-filled carbon nanotubes. Adapted from [135]. Copyright 2006 Elsevier.



4.3. Nanostructured tin oxide-carbon composites

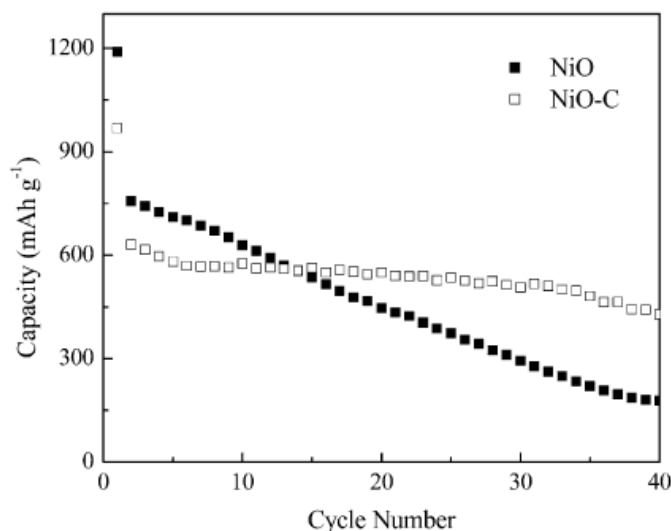
SnO₂ is a wide-band-gap ($E_g = 3.6$ V) n-type semiconductor which finds wide applications [138-140]. SnO₂ is an attractive anode material because SnO₂ can intercalate twice Li (781 mAh/g) compared to graphite [140-142]. However, the tin oxide anodes face the same problem of drastic volume change during cycling as the metallic tin electrodes [140,143]. The electrochemical performance of tin oxides can also be improved by forming composites with carbonaceous materials. The carbonaceous material serves as the buffering matrix to hinder the agglomeration of nanoparticles and enhance the electrical contact; it also delivers additional capacity at the same time [144-148]. In the work reported by Ning Du *et al.*, polycrystalline SnO₂ nanotubes have grown on the CNTs layer by layer [149]. These nanotube electrodes exhibit large reversible capacities due to the high specific surface area. SnO₂ can also be dispersed into multi-walled CNTs by using a one-step thioglycolic-acid-assisted wet chemical method [150] or through the oxidation process in supercritical carbon dioxide-methanol solution [151]. The thickness of SnO₂ coating can be controlled by changing pH value and hydrolysis time [150]. Hui Qiao *et al.* [152] and Yi-Chun Chen *et al.* [127] have both reported SnO₂-C composites with core-shell structures prepared by using a one-pot solvothermal method and a sol-gel method, respectively. The solvothermal method produces the SnO₂-C core-shell structure, and the sol-gel method yields the C-SnO₂ core-shell structure. Other SnO₂-C composites include SnO₂-C hollow spheres [153] and C-coated SnO₂ nanoparticles [154]. The C-coated SnO₂ nanoparticles deliver a discharge capacity of ~500 mAh/g over 20 cycles. Other than SnO₂-C composites, SnO-CNT composites have attracted some research interests and can be obtained via the sol-gel method [155]. The well-dispersed SnO can hinder or reduce the formation of the SEI film, which reduces the large capacity loss of pristine CNTs in the first cycle.

4.4. Nanostructured transition metal oxide-carbon composites

Apart from tin oxides, nanostructured transition-metal oxides such as TiO_2 , CuO , NiO , and Co_3O_4 can also be good candidates for anode materials [156]. These nanostructured oxide electrodes all deliver higher capacities than graphite-based anodes [2]. A variety of transition metal oxides can also form composites with carbonaceous materials. Here carbon is mainly used to improve the electric contact of the electrodes, in addition to acting as a buffering matrix for dispersing host materials.

Titanium oxide is a good host for lithium ions due to its high reversible capacity, low cost, and nontoxicity [157]. Another advantage offered by titanium oxide is higher operating voltage (~ 1.7 V vs. Li^+ (1M)/Li) than that of carbonaceous materials (~ 0.1 V vs. Li^+ (1M)/Li) [158]. TiO_2 provides facile diffusion paths for Li ions [159], but its electric conductivity is relatively low ($\sim 10^{-12}$ S/cm) [160], which leads to poor cycling stability [161]. A possible method to solve this problem is to combine TiO_2 with carbonaceous materials. The TiO_2 -carbon anodes demonstrate enhanced kinetics of lithiation/delithiation processes and increased diffusion coefficient of Li ions [159]. In the structure of TiO_2 -C core-shell composites synthesized by L.J. Fu *et al.*, the carbon shells enwrap the TiO_2 cores and hinder the agglomeration of nanoparticles [159]. A hydrothermal method followed by calcination [160] has been used to fabricate a composite of TiO_2 nanotubes and carbon in which nano-sized C is dispersed in TiO_2 . This composite is also a porous material with large surface area. The dispersed nano-sized carbon helps to reduce the bulk resistance, SEI resistance and charge transfer resistance in the anode. This composite material is able to maintain a discharge capacity of ~ 138 mAh/g over 70 cycles. Nanoporous TiO_2 -C composite can also be prepared by using a template method [161]. The conductive carbon network is coated onto the TiO_2 in this structure, which facilitates the transportation of Li ions and electrons.

Figure 9. capacity vs. cycle number profiles of the NiO and NiO-C electrodes cycled between 0.02 and 3.0 V at 0.1 C rate. Adapted from [162]. Copyright 2007 the Electrochemical Society.



Apart from TiO_2 , NiO has a theoretical capacity of 718 mAh/g. However, NiO suffers from aggregation, pulverization and poor conductivity [162]. Tu's group have synthesized NiO-C

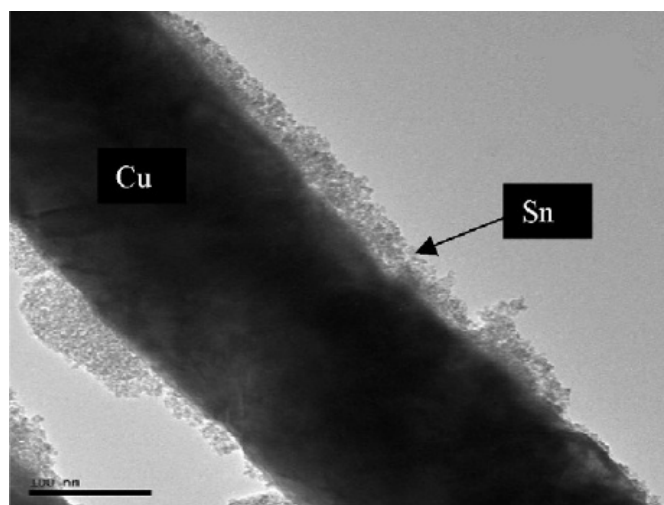
composites by carbonizing the net-structured [162] and spherical [163] NiO under hydrothermal condition. Carbon filled in the porous NiO stabilizes the structure and improves the electrical conductivity of NiO matrix. Figure 9 shows cycling performances of net-structured NiO and NiO-C nanocomposite electrodes at a current rate of 0.1 C. The composite electrodes retain a capacity of 429 mAh/g compared to that of 178 mAh/g for the NiO electrode over 40 cycles. Similar to NiO, CoO has a theoretical capacity of 715 mAh/g and the theoretical capacity of Co₃O₄ is 1100 mAh/g [156,164]. Nanostructured cobalt oxides containing CoO and Co₃O₄ can form composites with mesoporous carbon spheres [165]. The porous carbon provides good electric conductivity and buffer space, in addition to hindering the aggregation of the nanoparticles. Such an electrode delivers a capacity of 550 mAh/g after 30 cycles.

4.5. Other nanostructured composites

Nano-sized SnSb anodes also show high Li-ion intercalation capacities [117,166-168]. However, the nanoparticles with diameters less than 100 nm easily aggregate together, losing their advantage as nanomaterials and showing gradually decreased capacities due to the drastic volume change [167,168]. Xuejie Huang's group has dispersed SnSb nanoparticles on the rigid carbonaceous spherical material such as mesophase carbon microbeads (MCMB) and hard carbon spherules (HCS) to separate these nanoparticles [169-171]. The SnSb content should not exceed 30 wt% in the SnSb-MCMB composite, otherwise severe aggregation will appear again. The SnSb-HCS electrode shows a high coulombic efficiency (82%) in the first cycle, which is ascribed to the less surface area exposed to the electrolyte and thus less formation of the SEI film. The SnSb-HCS electrode shows a capacity of 460 mAh/g over 35 cycles at a current density of 0.2 mA/cm².

In addition to carbonaceous materials, materials that are electrochemically inert to Li can also serve as a ductile host matrix for Si [172,173]. TiN is not reactive with Li in the potential range of 0.02-1.2 V in terms of electrochemistry and is not reactive with Li and Si in terms of chemistry. It also has superior electrical conductivity and mechanical strength. The optimum milling time is 12 h in this research work. The electrodes with a milling time of 6 h show poor cycling stabilities due to poor binding between the two components [117]. On the other hand, milling with longer time (18 h) may generate inactive Si, and thus decreases the capacity of the electrode. Another alloy, nanocrystalline NiSi alloy, has been reported [172] to form the active/inactive composites, in which Si acts as the active center and Ni functions as the buffering matrix. Such an anode shows a discharge capacity of 1,180 mAh/g in the first cycle and retains 800 mAh/g after 25 cycles. Ni dispersed in Co₃O₄ can improve the initial coulombic efficiency. Mechanical milling has been used to synthesize Ni-Co₃O₄ composite [174]. The initial coulombic efficiency is enhanced from 69% for bare Co₃O₄ to 79%, which is ascribed to the optimum contact area of Co₃O₄ and Ni. Si-coated Cu nanopillars are another composites composed of the active component (Sn) and inactive component (Cu) and can be fabricated by a simple electroplating method [175]. This brush-like structure with large surface area can effectively alleviate the effect of volume change during cycling and improve the power rate performance. Figure 10 shows the TEM image of one "bristle" on the "brush" and the deposition time is 5 minutes. It is clear that a tin layer with the thickness in the range of 20-50 nm is deposited on the Cu pillar.

Figure 10. TEM image of a single Sn-covered Cu nanopillar (5 min tin deposition). Adapted from [176]. Copyright 2009 Elsevier.



5. Concluding Remarks

This review clearly reveals how moving from pristine materials to nanocomposite materials can significantly improve device performances for energy conversion and storage. The development of high-performance lithium-ion batteries can benefit from distinct properties of nanocomposites, such as excellent electric conductivity and freedom for volume change during Li-ion insertion/extraction process, as well as enhanced electrochemical, thermal and structural stability during charging/discharging cycles.

Applications of nanotechnology in energy storage are in the stage of research and development. For realization of wide industrial applications, further work is required to achieve controlled and large-scale synthesis of nanocomposite materials, to understand mechanisms of lithium storage in nanocomposite electrodes and kinetic transport on the interface between electrode and electrolyte. The effects of nanostructures in battery performance are not only simple consequences of a reduction in size or combination of two materials. Interfacial properties are subtle and critical. This challenges researchers worldwide to carry out systematic experimental studies and to develop predictive theoretical tools for better fundamental understanding of relationships between nanostructures and electrochemical characteristics of electrode materials.

Acknowledgments

C. C. would like to acknowledge the LSU Graduate School Enhancement Award.

References

1. Van Schalkwijk, W., Scrosati, B., Eds. *Advances in Lithium-Ion Batteries*; Springer: Berlin, Germany, 2002.

2. Tarascon, J.M.; Armand, M. Issues and challenges facing rechargeable lithium batteries. *Nature* **2001**, *414*, 359-367.
3. Cao, G.Z. *Nanostructures and Nanomaterials, Synthesis, Properties and Applications*; Imperial College Press: London, UK, 2004.
4. Reimers, J.N.; Dahn, J.R. Electrochemical and *in situ* X-ray diffraction studies of lithium intercalation in Li_xCoO_2 . *J. Electrochem. Soc.* **1992**, *139*, 2091-2097.
5. Kumta, P.N.; Gallet, D.; Waghray, A.; Blomgren, G.E.; Setter, M.P. Synthesis of LiCoO_2 powders for lithium-ion batteries from precursors derived by rotary evaporation. *J. Power Sources* **1998**, *72*, 91-98.
6. Ohzuku, T.; Ueda, A. Why transition metal (di) oxides are the most attractive materials for batteries. *Solid State Ionics* **1994**, *69*, 201-211.
7. Liu, H.; Li, C.; Zhang, H.P.; Fu, L.J.; Wu, Y.P.; Wu, H.Q. Kinetic study on LiFePO_4/C nanocomposites synthesized by solid state technique. *J. Power Sources* **2006**, *159*, 717-720.
8. Takahara, H.; Takeuchi, T.; Tabuchi, M.; Kageyama, H.; Kobayashi, Y.; Kurisu, Y.; Kondo, S.; Kanno, R. All-solid-state lithium secondary battery using oxysulfide glass. *J. Electrochem. Soc.* **2004**, *151*, A1539-A1544.
9. Cao, Q.; Zhang, H.P.; Wang, G.J.; Xia, Q.; Wu, Y.P.; Wu, H.Q. A novel carbon-coated LiCoO_2 as cathode material for lithium ion battery. *Electrochem. Commun.* **2007**, *9*, 1228-1232.
10. Li, G.; Yang, Z.X.; Yang, W.S. Effect of FePO_4 coating on electrochemical and safety performance of LiCoO_2 as cathode material for Li-ion batteries. *J. Power Sources* **2008**, *183*, 741-748.
11. Kim, J.; Noh, M.; Cho, J.; Kim, H.; Kim, K. Controlled nanoparticle metal phosphates (Metal = Al, Fe, Ce, and Sr) coatings on LiCoO_2 cathode materials. *J. Electrochem. Soc.* **2005**, *1526*, A1142-A1148.
12. Cho, J.; Kim, B.; Lee, J.; Kim, Y.; Park, B. Annealing-temperature effect on various cutoff-voltage electrochemical performances in AlPO_4 -nanoparticle-coated LiCoO_2 . *J. Electrochem. Soc.* **2005**, *1521*, A32-A36.
13. Kim, B.; Kim, C.; Kim, T.; Ahn, D.; Park, B. The effect of AlPO_4 -coating layer on the electrochemical properties in LiCoO_2 thin films. *J. Electrochem. Soc.* **2006**, *1539*, A1773-A1777.
14. Kim, Y.J.; Cho, J.; Kim, T.-J.; Park, B. Suppression of cobalt dissolution from the LiCoO cathodes with various metal-oxide coatings. *J. Electrochem. Soc.* **2003**, *150*, A1723-A1725.
15. Lui, L.; Wang, Z.; Li, H.; Chen, L.; Huang, X. Al_2O_3 -coated LiCoO_2 as cathode material for lithium ion batteries. *Solid State Ionics* **2002**, *152-153*, 341-346.
16. Cho, J.; Kim, C.-S.; Yoo, S.-I. Improvement of structural stability of LiCoO_2 cathode during electrochemical cycling by sol-gel coating of SnO_2 . *Electrochem. Solid-State Lett.* **2000**, *3*, 362-365.
17. Wang, Z.; Huang, X.; Chen, L. Performance improvement of surface-modified LiCoO_2 cathode materials: an infrared absorption and X-ray photoelectron spectroscopic investigation. *J. Electrochem. Soc.* **2003**, *150*, A199-A208.
18. Fang, T.; Duh, J.; Sheen, S. Improving the electrochemical performance of LiCoO_2 cathode by nanocrystalline ZnO coating. *J. Electrochem. Soc.* **2005**, *152*, A1701-A1706.

19. Chung, K.Y.; Yoon, W.; McBreen, J.; Yang, X.; Oh, S.H.; Shin, H.C.; Cho, W.I.; Cho, B.W. Structural studies on the effects of ZrO_2 coating on LiCoO_2 during cycling using *in situ* X-ray diffraction technique. *J. Electrochem. Soc.* **2006**, *153*, A2152-A2157.
20. Miyashiro, H.; Yamanaka, A.; Tabuchi, M.; Seki, S.; Nakayama, M.; Ohno, Y.; Kobayashi, Y.; Mita, Y.; Usami, A.; Wakihara, M. Improvement of degradation at elevated temperature and at high state-of-charge storage by ZrO_2 coating on LiCoO_2 . *J. Electrochem. Soc.* **2006**, *153*, A348-A353.
21. Lu, C.-Z.; Chen, J.-M.; Cho, Y.-D.; Hsu, W.-H.; Muralidharan, P.; Fey, G.T.-K. Electrochemical performance of LiCoO_2 cathodes by surface modification using lanthanum aluminum garnet. *J. Power Sources* **2008**, *184*, 392-401.
22. Ohta, N.; Takada, K.; Zhang, L.; Ma, R.; Osada, M.; Sasaki, T. Enhancement of the high-rate capability of solid-state lithium batteries by nanoscale interfacial modification. *Adv. Mater.* **2006**, *18*, 2226-2229.
23. Fey, G.T.-K.; Huang, C.-F.; Muralidharan, P.; Chang, E.S.-S. Improved electrochemical performance of LiCoO_2 surface treated with $\text{Li}_4\text{Ti}_5\text{O}_{12}$. *J. Power Sources* **2007**, *174*, 1147-1151.
24. Wang, H.; Zhang, W.-D.; Zhu, L.-Y.; Chen, M.-C. Effect of LiFePO_4 coating on electrochemical performance of LiCoO_2 at high temperature. *Solid State Ionics* **2007**, *178*, 131-136.
25. Abello, L.; Husson, E.; Repelin, Y. R.; Lucazeau, G. Vibrational spectra and valence force field of crystalline V_2O_5 . *Spectrochim. Acta* **1983**, *39A*, 641-651.
26. Sun, Y.; Hong, K.; Prakash, J. The Effect of ZnO coating on electrochemical cycling behavior of spinel LiMn_2O_4 cathode materials at elevated temperature. *J. Electrochem. Soc.* **2003**, *150*, A970-A972.
27. Liu, D.Q.; Liu, X.Q.; He, Z.Z. Surface modification by ZnO coating for improving the elevated temperature performance of LiMn_2O_4 . *J. Alloys Compd.* **2007**, *436*, 387-391.
28. Han, J.; Myung, S.; Sun, Y. Improved electrochemical cycling behavior of ZnO -coated $\text{Li}_{1.05}\text{Al}_{0.1}\text{Mn}_{1.85}\text{O}_{3.95}\text{F}_{0.05}$ Spinel at 55 °C. *J. Electrochem. Soc.* **2006**, *153*, A1290-A1295.
29. Thackeray, M.M.; Johnson, C.S.; Kim, J.S.; Lauzze, K.C.; Vaughey, J.T.; Dietz, N.; Abraham, D.; Hackney, S.A.; Zeltner, W.; Anderson, M.A. ZrO_2 - and Li_2ZrO_3 -stabilized spinel and layered electrodes for lithium batteries. *Electrochem. Commun.* **2003**, *5*, 752-758.
30. Kim, J.S.; Johnson, C.S.; Vaughey, J.T.; Hackney, S.A.; Walz, K.A.; Zeltner, W.A.; Anderson, M.A.; Thackeray, M.M. The electrochemical stability of spinel electrodes coated with ZrO_2 , Al_2O_3 , and SiO_2 from colloidal suspensions. *J. Electrochem. Soc.* **2004**, *151*, A1755-A1761.
31. Takai, S.; Kamata, M.; Fujine, S.; Yoneda, K.; Kanda, K.; Esaka, T. Diffusion coefficient measurement of lithium ion in sintered $\text{Li}_{1.33}\text{Ti}_{1.67}\text{O}_4$ by means of neutron radiography. *Solid State Ionics* **1999**, *123*, 165-172.
32. Ohzuku, T.; Ueda, A.; Yamadoto, N. Zero-strain insertion material of $\text{Li}[\text{Li}_{1/3}\text{Ti}_{5/3}]\text{O}_4$ for rechargeable lithium cells. *J. Electrochem. Soc.* **1995**, *142*, 1431-1435.
33. Li, D.-Q.; Liu, X.-Q.; He, Z.-Z. The elevated temperature performance of LiMn_2O_4 coated with $\text{Li}_4\text{Ti}_5\text{O}_{12}$ for lithium ion battery. *Mater. Chem. Phys.* **2007**, *105*, 362-366.
34. Biensan, Ph.; Simon, B.; Pérès, J.P.; de Guibert, A.; Broussely, M.; Bodet, J.M.; Pertion, F. On safety of lithium-ion cells. *J. Power Sources* **1999**, *81-82*, 906-912.

35. Zhang, Z.R.; Li, J.; Yang, Y. The effects of decomposition products of electrolytes on the thermal stability of bare and TiO₂-coated delithiated Li_{1-x}Ni_{0.8}Co_{0.2}O₂ cathode materials. *Electrochim. Acta* **2006**, *52*, 1442-1450.
36. Omanda, H.; Brousse, T.; Marhic, C.; Schleich, D.M. Improvement of the thermal stability of LiNi_{0.8}Co_{0.2}O₂ cathode by a SiO_x protective coating. *J. Electrochem. Soc.* **2004**, *151*, A922-A929.
37. Xiang, J.F.; Chang, C.X.; Yuan, L.J.; Sun, J.T. A simple and effective strategy to synthesize Al₂O₃-coated LiNi_{0.8}Co_{0.2}O₂ cathode materials for lithium ion battery. *Electrochem. Commun.* **2008**, *10*, 1360-1363.
38. Hu, G.-R.; Deng, X.-R.; Peng, Z.-D.; Du, K. Comparison of AlPO₄- and Co₃(PO₄)₂-coated LiNi_{0.8}Co_{0.2}O₂ cathode materials for Li-ion battery. *Electrochim. Acta* **2008**, *53*, 2567-2573.
39. Hu, S.-K.; Cheng, G.-H.; Cheng, M.-Y.; Hwang, B.-J.; Santhanam, R. Cycle life improvement of ZrO₂-coated spherical LiNi_{1/3}Co_{1/3}Mn_{1/3}O₂ cathode material for lithium ion batteries. *J. Power Sources* **2009**, *188*, 564-569.
40. Franger, S.; Cras, F.L.; Bourbon, C.; Rouault, H. LiFePO₄ Synthesis routes for enhanced electrochemical performance. *Electrochem. Solid-State Lett.* **2002**, *5*, A231-A233.
41. Prosini, P.P.; Lisi, M.; Zane, D.; Pasquali, M. Determination of the chemical diffusion coefficient of lithium in LiFePO₄. *Solid State Ionics* **2002**, *148*, 45-51.
42. Yu, D.Y.W.; Fietzek, C.; Weydanz, W.; Donoue, K.; Inoue, T.; Kurokawa, H.; Fujitani, S. Study of LiFePO₄ by cyclic voltammetry. *J. Electrochem. Soc.* **2007**, *154*, A253-A257.
43. Chung, S.-Y.; Bloking, J.T.; Chiang, Y.-M. Electronically conductive phospho-olivines as lithium storage electrodes. *Nat. Mater.* **2002**, *1*, 123-128.
44. Yang, S.; Song, Y.; Ngala, K.; Zavalij, P.Y.; Whittingham, M.S. Performance of LiFePO₄ as lithium battery cathode and comparison with manganese and vanadium oxides. *J. Power Sources* **2003**, *119*, 239-246.
45. Ravet, N.; Goodenough, J.B.; Besner, S.; Simoneau, M.; Hovington, P.; Armand, M.; *Electrochem. Soc. Abstr.* **1999**, *99*, 127.
46. Ravet, N.; Besner, S.; Simoneau, M.; Valle'e, A.; Armand, M.; Magnan, J.-F. Matériaux d'électrode présentant une conductivité de surface élevée. *European Patent 1049182A2*, 2000.
47. Yang, S.; Zavalij, P.Y.; Whittingham, M.S. Hydrothermal synthesis of lithium iron phosphate cathodes. *Electrochem. Commun.* **2001**, *3*, 505-508.
48. Spong, A.D.; Vitins, G.; Owen, J.R. A solution-precursor synthesis of carbon-coated LiFePO₄ for Li-ion cells. *J. Electrochem. Soc.* **2005**, *152*, A2376-A2382.
49. Nakamura, T.; Miwa, Y.; Tabuchi, M.; Yamada, Y. Structural and surface modifications of LiFePO₄ olivine particles and their electrochemical properties. *J. Electrochem. Soc.* **2006**, *153*, A1108-A1114.
50. Nakano, H.; Dokko, K.; Koizumi, S.; Tannai, H.; Kanamuraa, K. Hydrothermal synthesis of carbon-coated LiFePO₄ and its application to lithium polymer battery. *J. Electrochem. Soc.* **2008**, *155*, A909-A914.
51. Gaberscek, M.; Dominko, R.; Bele, M.; Remskar, M.; Hanzel, D.; Jamnik, J. Porous carbon-decorated LiFePO₄ prepared by sol-gel method based on citric acid. *J. Solid State Ionics* **2005**, *176*, 1801-1805.

52. Kim, J.-K.; Cheruvally, G.; Ahn, J.-H.; Hwang, G.-C.; Choi, J.-B. Electrochemical properties of carbon-coated LiFePO₄ synthesized by a modified mechanical activation process. *J. Phys. Chem. Solids* **2008**, *69*, 2371-2377.
53. Konarova, M.; Taniguchi, I. Preparation of carbon coated LiFePO₄ by a combination of spray pyrolysis with planetary ball-milling followed by heat treatment and their electrochemical properties. *Powder Technol.* **2009**, *191*, 111-116.
54. Kim, K.; Jeong, J.H.; Kim, I.-J.; Kim, H.-S. Carbon coatings with olive oil, soybean oil and butter on nano-LiFePO₄. *J. Power Sources* **2007**, *167*, 524-528.
55. Wilcox, J.D.; Doeff, M.M.; Marcinek, M.; Kostecki, R. Factors influencing the quality of carbon coatings on LiFePO₄. *J. Electrochem. Soc.* **2007**, *154*, A389-A395.
56. Dominko, R.; Goupil, J.M.; Bele, M.; Gaberscek, M.; Remskar, M.; Hanzel, D.; Jamnik, J. Impact of LiFePO₄/C composites porosity on their electrochemical performance. *J. Electrochem. Soc.* **2005**, *152*, A858-A863.
57. Croce, F.; Epifanio, A.D.; Hassoun, J.; Deptula, A.; Olczac, T.; Scrosati, B. A novel concept for the synthesis of an improved LiFePO₄ lithium battery cathode. *Electrochem. Solid-State Lett.* **2002**, *5*, A47-A50.
58. León, B.; Vicente, C. Pérez; Tirado, J.L.; Biensan, Ph.; Tessier, C. Optimized chemical stability and electrochemical performance of LiFePO₄ composite materials obtained by ZnO coating. *J. Electrochem. Soc.* **2008**, *155*, A211-A216.
59. Rho, Y.-H.; Nazar, L.F.; Perry, L.; Ryan, D. Surface chemistry of LiFePO₄ studied by Mössbauer and X-ray photoelectron spectroscopy and its effect on electrochemical properties. *J. Electrochem. Soc.* **2007**, *154*, A283-A289.
60. Xie, H.-M.; Wang, R.-S.; Ying, J.-R.; Zhang, L.-Y.; Jalbout, A.F.; Yu, H.-Y.; Yang, G.-L.; Pan, X.-M.; Su, Z.-M. Optimized LiFePO₄-polyacene cathode material for lithium-ion batteries. *Adv. Mater.* **2006**, *18*, 2609-2613.
61. Huanzg, Y.-H.; Park, K.-S.; Goodenough, J.B. Improving lithium batteries by tethering carbon-coated LiFePO₄ to polypyrrole. *J. Electrochem. Soc.* **2006**, *153*, A2282-A2286.
62. Huang, Y.-H.; Goodenough, J.B. High-rate LiFePO₄ lithium rechargeable battery promoted by electrochemically active polymers. *Chem. Mater.* **2008**, *20*, 7237-7241.
63. Hu, Y.-S.; Guo, Y.-G.; Dominko, R.; Gaberscek, M.; Jamnik, J. Improved electrode performance of porous LiFePO₄ Using RuO₂ as an oxidic nanoscale interconnect. *Adv. Mater.* **2007**, *19*, 1963-1966.
64. Huang, H.; Yin, S.-C.; Nazar, L.F. Approaching theoretical capacity of LiFePO₄ at room temperature at high rates. *Electrochem. Solid-State Lett.* **2001**, *4*, A170-A172.
65. Hsu, K.-F.; Tsay, S.-Y.; Hwang, B.-J. Synthesis and characterization of nano-sized LiFePO₄ cathode materials prepared by a citric acid-based sol-gel route. *J. Mater. Chem.* **2004**, *14*, 2690-2696.
66. Padhi, K.; Nanjundaswamy, K.S.; Goodenough, J.B. Phospho-olivines as positive-electrode materials for rechargeable lithium batteries. *J. Electrochem. Soc.* **1997**, *144*, 1188-1194.
67. Herle, P.S.; Ellis, B.; Coombs, N.; Nazar, L.F. Nano-network electronic conduction in iron and nickel olivine phosphates. *Nat. Mater.* **2004**, *3*, 147-152.

68. Tarascon, J.M.; Delacourt, C.; Prakash, A.S.; Morcrette, M.; Hegde, M.S.; Wurm, C.; Masquelier, C. Various strategies to tune the ionic/electronic properties of electrode materials. *Dalton Trans.* **2004**, *19*, 2988-2994.
69. Murphy, D.W.; Christian, P.A.; DiSalvo, F.J.; Waszczak, J.V. Lithium incorporation by vanadium pentoxide. *Inorg. Chem.* **1979**, *18*, 2800-2803.
70. Whittingham, M.S. The role of ternary phases in cathode reactions. *J. Electrochem. Soc.* **1976**, *123*, 315-320.
71. Koltypin, M.; Pol, V.; Gedanken, A.; Aurbach, D. The study of carbon-coated V_2O_5 nanoparticles as a potential cathodic material for Li rechargeable batteries. *J. Electrochem. Soc.* **2007**, *154*, A605-A613.
72. Sakamoto, J.S.; Dunn, B. Vanadium oxide-carbon nanotube composite electrodes for use in secondary lithium batteries. *J. Electrochem. Soc.* **2002**, *149*, A26-A30.
73. Kuwahara, A.; Suzuki, S.; Miyayama, M. Estimation of high-rate discharge capacities in V_2O_5 /carbon composite electrodes. *Solid State Ionics* **2008**, *179*, 1890-1896.
74. Dubarry, D.; Gaubicher, J.; Moreau, P.; Guyomard, D. Formation of $Li_{1+n}V_3O_8/\beta-Li_{1/3}V_2O_5/C$ nanocomposites by carboreduction and the resulting improvement in Li capacity retention. *J. Electrochem. Soc.* **2006**, *153*, A295-A300.
75. Reddy, A.L.M.; Shaijumon, M.M.; Gowda, S.R.; Ajayan, P.M. Coaxial MnO_2 /carbon nanotube array electrodes for high-performance lithium batteries. *Nano Lett.* **2009**, *9*, 1002-1006.
76. Huang, X.; Yue, H.; Attia, A.; Yang, Y. Preparation and properties of manganese oxide/carbon composites by reduction of potassium permanganate with acetylene black. *J. Electrochem. Soc.* **2007**, *154*, A26-A33.
77. Kawaoka, H.; Hibino, M.; Zhou, H.; Honma, I. Optimization of sonochemical synthesis condition of manganese oxide/acetylene black nanocomposite for high power lithium-ion batteries. *J. Electrochem. Soc.* **2005**, *152*, A1217-A1220.
78. Yang, J.; Xu, J.J. Synthesis and characterization of carbon-coated lithium transition metal phosphates $LiMPO_4$ ($M = Fe, Mn, Co, Ni$) prepared via a nonaqueous sol-gel route. *J. Electrochem. Soc.* **2006**, *153*, A716-A723.
79. Huang, H.; Yin, S.-C.; Kerr, T.; Taylor, N.; Nazar, L.F. Nanostructured composites: A high capacity, fast rate $Li_3V_2(PO_4)_3$ /carbon cathode for rechargeable lithium batteries. *Adv. Mater.* **2002**, *14*, 1525-1528.
80. Shiraishi, K.; Dokko, K.; Kanamura, K.. Formation of impurities on phospho-olivine $LiFePO_4$ during hydrothermal synthesis. *J. Power Sources* **2005**, *146*, 555-558.
81. Myung, S.T.; Komaba, S.; Hirosaki, N.; Yashiro, H.; Kumagai, N. Emulsion drying synthesis of olivine $LiFePO_4/C$ composite and its electrochemical properties as lithium intercalation material. *Electrochim. Acta* **2004**, *49*, 4213-4222.
82. Chen, Z.-Y.; Zhu, H.-L.; Ji, S.; Fakir, R.; Linkov, V. Influence of carbon sources on electrochemical performances of $LiFePO_4/C$ composites. *Solid State Ionics* **2008**, *179*, 1810-1815.
83. Jin, B.; Jin, E.M.; Park, K.-H.; Gu, H.-B. Electrochemical properties of $LiFePO_4$ -multiwalled carbon nanotubes composite cathode materials for lithium polymer battery. *Electrochem. Commun.* **2008**, *10*, 1537-1540.

84. Barker, J.; Saïdi, M.Y.; Swoyer, J.L. Lithium Iron(II) phospho-olivines prepared by a novel carbothermal reduction method. *Electrochem. Solid State Lett.* **2003**, *6*, A53-A55.
85. Saïdi, M.Y.; Huang, H.; Swoyer, J.L.; Adamson, G. Performance characteristics of lithium vanadium phosphate as a cathode material for lithium-ion batteries. *J. Power Sources* **2003**, *119-121*, 266-272.
86. Ren, M.M.; Zhou, Z.; Li, Y.Z.; Gao, X.P.; Yan, J. Preparation and electrochemical studies of Fe-doped $\text{Li}_3\text{V}_2(\text{PO}_4)_3$ cathode materials for lithium-ion batteries. *J. Power Sources* **2006**, *162*, 1357-1362.
87. Fu, P.; Zhao, Y.M.; Dong, Y.Z.; An, X.N.; Shen, G.P. Synthesis of $\text{Li}_3\text{V}_2(\text{PO}_4)_3$ with high performance by optimized solid-state synthesis routine. *J. Power Sources* **2006**, *162*, 651-657.
88. Li, Y.Z.; Zhou, Z.; Ren, M.M.; Gao, X.P.; Yan, J. Electrochemical performance of nanocrystalline $\text{Li}_3\text{V}_2(\text{PO}_4)_3$ /carbon composite material synthesized by a novel sol-gel method. *Electrochim. Acta* **2006**, *51*, 6498-6502.
89. Fu, P.; Zhao, Y.M.; An, X.N.; Dong, Y.Z.; Hou, X.M. Structure and electrochemical properties of nanocarbon-coated $\text{Li}_3\text{V}_2(\text{PO}_4)_3$ prepared by sol-gel method. *Electrochim. Acta* **2007**, *52*, 5281-5285.
90. Yabuuchi, N.; Ohzuku, T. Novel lithium insertion material of $\text{LiCo}_{1/3}\text{Ni}_{1/3}\text{Mn}_{1/3}\text{O}_2$ for advanced lithium-ion batteries. *J. Power Sources* **2003**, *119-121*, 171-174.
91. Lin, B.; Wen, Z.Y.; Han, J.D.; Wu, X.W. Electrochemical properties of carbon-coated $\text{Li}[\text{Ni}_{1/3}\text{Co}_{1/3}\text{Mn}_{1/3}]\text{O}_2$ cathode material for lithium-ion batteries. *Solid State Ionics* **2008**, *179*, 1750-1753.
92. Kim, H.-S.; Kim, K.; Moon, S.-I.; Kim, I.-J.; Gu, H.-B. A study on carbon-coated $\text{LiNi}_{1/3}\text{Mn}_{1/3}\text{Co}_{1/3}\text{O}_2$ cathode material for lithium secondary batteries. *J. Solid State Electrochem.* **2008**, *12*, 867-872.
93. Boyano, I.; Bengoechea, M.; de Meatza, I.; Miguel, O.; Cantero, I.; Ochoteco, E.; Rodríguez, J.; Lira-Cantú, M.; Gómez-Romero, P. Improvement in the Ppy/ V_2O_5 hybrid as a cathode material for Li ion batteries using PSA as an organic additive. *J. Power Sources* **2007**, *166*, 471-477.
94. Ferreira, M.; Zucolotto, V.; Huguenin, F.; Torresi, R.M.; Oliveira, O.N., Jr. Layer-by-Layer nanostructured hybrid films of polyaniline and vanadium oxide. *J. Nanosci. Nanotechnol.* **2002**, *2*, 29-32.
95. Huguenin, F.; dos Santos, D.S., Jr.; Bassi, A.; Nart, F. C.; Oliveira, Jr. O. N. Charge storage capability in nanoarchitectures of V_2O_5 /chitosan/poly(ethylene oxide) produced using the Layer-by-Layer technique. *Adv. Funct. Mater.* **2004**, *14*, 985-991.
96. Ponzio, E.A.; Benedetti, T.M.; Torresi, R.M. Electrochemical and morphological stabilization of V_2O_5 nanofibers by the addition of polyaniline. *Electrochim. Acta* **2007**, *52*, 4419-4427.
97. Reddy, C.V.S.; Jin, W.; Zhu, Q.-Y.; Chen, W.; Kalluru, R.R. Polymer intercalated V_2O_5 nanostructured cathodes for secondary batteries. *Eur. Phys. J. Appl. Phys.* **2007**, *38*, 31-35.
98. Olivetti, E.A.; Kim, J.H.; Sadoway, D.R.; Asatekin, A.; Mayes, A.M. Sol-gel synthesis of vanadium oxide within a block copolymer matrix. *Chem. Mater.* **2006**, *18*, 2828-2833.
99. Guy, D.; Lestriez, B.; Guyomard, D. New composite electrode architecture and improved battery performance from the smart use of polymers and their properties. *Adv. Mater.* **2004**, *16*, 553-557.

100. Peter, N.; Klaus, M.; Santhannam, K.S.V.; Otto, H. Electrochemically active polymers for rechargeable batteries. *Chem. Rev.* **1997**, *97*, 207-282.
101. Wang, J.; Yang, J.; Xie, J.; Xu, N. A novel conductive polymer-sulfur composite cathode material for rechargeable lithium batteries. *Adv. Mater.* **2002**, *14*, 963-965.
102. Wang, J.; Yang, J.; Wan, C.; De, K.; Xie, J.; Xu, N. Sulfur composite cathode materials for rechargeable lithium batteries. *Adv. Funct. Mater.* **2003**, *13*, 487-492.
103. Park, K.-S.; Schougaard, S.B.; Goodenough, J.B. Conducting-polymer/iron-redox-couple composite cathodes for lithium secondary batteries. *Adv. Mater.* **2007**, *19*, 848-851.
104. Takahashi, K.; Wang, Y.; Cao, G.Z. Ni-V₂O₅·nH₂O core-shell nanocable arrays for enhanced electrochemical intercalation. *J. Phys. Chem. B* **2005**, *109*, 48-51.
105. Wang, Y.; Lee, K.; Shang, H.; Wiley, B.; Xia, Y.; Cao, G. Ag-Ag_{0.08}V₂O₅·nH₂O composite films as host materials for Li⁺ intercalation. *Phys. Status Solidi A* **2005**, *202*, R79-R81.
106. Ghosh, P.; Mahanty, S.; Basu, R.N. Effect of silver addition on the properties of combustion synthesized nanocrystalline LiCoO₂. *Mater. Chem. Phys.* **2008**, *110*, 406-410.
107. Wook, J.S.; Lee, S.-M. LiCoO₂/Ag multilayer film cathodes for thin-film rechargeable lithium batteries. *J. Electrochem. Soc.* **2007**, *154*, A22-A25.
108. Guo, R.; Shi, P.F.; Cheng, X.Q.; Ma, Y.L.; Tan, Z. Effect of Ag additive on the performance of LiNi_{1/3}Co_{1/3}Mn_{1/3}O₂ cathode material for lithium ion battery. *J. Power Sources*, **2009**, *189*, 2-8.
109. Zhou, W.-J.; He, B.-L.; Li, H.-L. Synthesis structure and electrochemistry of Ag-modified LiMn₂O₄ cathode materials for lithium-ion batteries. *Mater. Res. Bull.* **2008**, *43*, 2285-2294.
110. Li, Y.; Kunitake, T.; Aoki, Y. Synthesis and Li⁺ intercalation/extraction in ultrathin V₂O₅ layer and freestanding V₂O₅/Pt/PVA multilayer films. *Chem. Mater.* **2007**, *19*, 575-580.
111. Imachi, N.; Takano, Y.; Fujimoto, H.; Kida, Y.; Fujitani, S. Layered cathode for improving safety of Li-ion batteries. *J. Electrochem. Soc.* **2007**, *154*, A412-A416.
112. Sivakkumar, S.R.; MacFarlane, R.D.; Forsyth, M.; Kim, D.-W. Ionic liquid-based rechargeable lithium metal-polymer cells assembled with polyaniline/carbon nanotube composite cathode. *J. Electrochem. Soc.* **2007**, *154*, A834-A838.
113. Sharma, R.A.; Seefurth, R.N. Thermodynamic properties of the lithium-silicon system. *J. Electrochem. Soc.* **1976**, *123*, 1763-1768.
114. Boukamp, B.A.; Lesh, G.C.; Huggins, R.A. All-solid lithium electrodes with mixed-conductor matrix. *J. Electrochem. Soc.* **1981**, *128*, 725-729.
115. Winter, M.; Besenhard, J.O.; Spahr, M.E.; Novak, P. Insertion electrode materials for rechargeable lithium batteries. *Adv. Mater.* **1998**, *10*, 725-763.
116. Kasavajjula, U.; Wang, C.; Appleby, A.J. Nano- and bulk-silicon-based insertion anodes for lithium-ion secondary cells. *J. Power Sources* **2007**, *163*, 1003-1039.
117. Li, H.; Huang, X.J.; Chen, L.Q.; Wu, Z.G.; Liang, Y. A high capacity nano-Si composite anode material for lithium rechargeable batteries. *Electrochem. Solid-State Lett.* **1999**, *2*, 547-549.
118. Zhang, Y.; Zhang, X.G.; Zhang, H.L.; Zhao, Z.G.; Li, F.; Liu, C.; Cheng, H.M. Composite anode material of silicon/graphite/carbon nanotubes for Li-ion batteries. *Electrochim. Acta* **2006**, *51*, 4994-5000.
119. Wang, G.X.; Ahn, J.H.; Yao, J.; Bewlay, S.; Liu, H.K. Nanostructured Si-C composite anodes for lithium-ion batteries. *Electrochem. Commun.* **2004**, *6*, 689-692.

120. Wilson, A.M.; Dahn, J.R. Lithium insertion in carbons containing nanodispersed silicon. *J. Electrochem. Soc.* **1995**, *142*, 326-332.
121. Shu, J.; Li, H.; Yang, R.Z.; Shi, Y.; Huang, X.J. Cage-like carbon nanotubes/Si composite as anode material for lithium ion batteries. *Electrochem. Commun.* **2006**, *8*, 51-54.
122. Wang, C.S.; Wu, G.T.; Zhang, X.B.; Qi, Z.F.; Li, W.Z. Lithium insertion in carbon-silicon composite materials produced by mechanical milling. *J. Electrochem. Soc.* **1998**, *145*, 2751-2758.
123. Endo, M.; Hayashi, T.; Kim, Y.A.; Tantrakarn, K.; Yanagisawa, T.; Dresselhaus, M.S. Nanofiber toughened polyethylene composites. *Carbon* **2004**, *42*, 2329-2331.
124. Khomenko, V.; Frackowiak, E.; Beguin, F. Determination of the specific capacitance of conducting polymer/nanotubes composite electrodes using different cell configurations. *Electrochem. Acta* **2005**, *50*, 2499-2506.
125. He, X.J.; Du, J.H.; Ying, Z.; Cheng, H.M. Positive temperature coefficient effect in multiwalled carbon nanotube/high-density polyethylene composites. *Appl. Phys. Lett.* **2005**, *86*, 062112.
126. Lee, H.-Y.; Lee, S.-M. Carbon-coated nano-Si dispersed oxides/graphite composites as anode material for lithium ion batteries. *Electrochem. Commun.* **2004**, *6*, 465-469.
127. Chen, Y.-C.; Chen, J.-M.; Huang, Y.-H.; Lee, Y.-R.; Shih, H.C. Size effect of tin oxide nanoparticles on high capacity lithium battery anode materials. *Surf. Coat. Technol.* **2007**, *202*, 1313-1318.
128. Derrien, G.; Hassoun, J.; Panero, S.; Scrosati, B. Nanostructured Sn-C composite as an advanced anode material in high-performance lithium-ion batteries. *Adv. Mater.* **2007**, *19*, 2336-2340.
129. Zhang, T.; Fu, L.J.; Gao, J.; Wua, Y.P.; Holze, R.; Wu, H.Q. Nanosized tin anode prepared by laser-induced vapor deposition for lithium ion battery. *J. Power Sources* **2007**, *174*, 770-773.
130. Guo, B.K.; Shu, J.; Tang, K.; Bai, Y.; Wang, Z.X.; Chen, L.Q. Nano-Sn/hard carbon composite anode material with high-initial coulombic efficiency. *J. Power Sources* **2008**, *177*, 205-210.
131. Dahn, J.R.; Zheng, T.; Liu, Y.; Xue, J.S. Mechanisms for lithium insertion in carbonaceous materials. *Science* **1995**, *270*, 590-593.
132. Withers, J.C.; Loufty, R.O.; Lowe, T.P. Fullerene commercial vision. *Fullerene Sci. Technol.* **1997**, *5*, 1-31.
133. Nalimova, V.A.; Skovsky, D.F.; Bondarenko, G.N.; Alvergnt-Gaucher, H.; Bonamy, G.; Beguin, F. Lithium interaction with carbon nanotubes. *Synth. Met.* **1997**, *88*, 89-93.
134. Wu, G.T.; Wang, C.S.; Zhang, X.B.; Yang, H.S.; Qi, Z.F.; He, P.M.; Li, W.Z. Structure and lithium insertion properties of carbon nanotubes. *J. Electrochem. Soc.* **1999**, *146*, 1696-1701.
135. Prem Kumar, T.; Ramesh, R.; Lin, Y.Y.; Fey, G.T.-K. Tin-filled carbon nanotubes as insertion anode materials for lithium-ion batteries. *Electrochem. Commun.* **2004**, *6*, 520-525.
136. Noh, M.J.; Kwon, Y.J.; Lee, H.J.; Cho, J.; Kim, Y.J.; Kim, M.G. Amorphous carbon-coated tin anode material for lithium secondary battery. *Chem. Mater.* **2005**, *17*, 1926-1929.
137. Morishita, T.; Hirabayashi, T.; Okuni, T.; Ota, N.; Inagaki, M. Preparation of carbon-coated Sn powders and their loading onto graphite flakes for lithium ion secondary battery. *J. Power Sources* **2006**, *160*, 638-644.

138. Wang, Y.; Jiang, X.; Xia, Y. A solution-phase, precursor route to polycrystalline SnO₂ nanowires that can be used for gas sensing under ambient conditions. *J. Am. Chem. Soc.* **2003**, *125*, 16176-16177.
139. Law, M.; Kind, H.; Messer, B.; Kim, F.; Yang, P. Photochemical sensing of NO₂ with SnO₂ nanoribbon nanosensors at room temperature. *Angew. Chem. Int. Ed.* **2002**, *41*, 2405-2408.
140. Idota, Y.; Kubota, T.; Matsufuji, A.; Maekawa, Y.; Miyasaka, T. Tin-based amorphous oxide: A high-capacity lithium-ion-storage material. *Science* **1997**, *276*, 1395-1397.
141. Idota, Y.; Mishima, M.; Miyaki, M.; Kubota, T.; Miyasaka, T. Nonaqueous secondary battery. *Eur. Pat. Appl.* **1995**, EP0651450 (A1).
142. Tahara, K.; Ishikawa, H.; Iwasaki, F.; Yahagi, S.; Sakkata, A.; Sakai, T. Non-aqueous electrolyte secondary battery and its production method. *Eur. Pat. Appl.* **1994**, EP0582173 (A1).
143. Besenhard, J. O.; Yang, J.; Winter, M. Will advanced lithium-alloy anodes have a chance in lithium-ion batteries? *J. Power Sources* **1997**, *68*, 87-90.
144. Lee, K.T.; Jung Y.S.; Oh, S.M. Synthesis of tin-encapsulated spherical hollow carbon for anode material in lithium secondary batteries. *J. Am. Chem. Soc.* **2003**, *125*, 5652-5653.
145. Sun, X.; Liu J.; Li, Y. Oxides@C core-shell nanostructures: One-pot synthesis, rational conversion, and Li storage property. *Chem. Mater.* **2006**, *18*, 3486-3494.
146. Park, M.S.; Kang, Y.M.; Kim, J.H.; Wang, G.X.; Dou, S.X.; Liu, H.K. Effects of low-temperature carbon encapsulation on the electrochemical performance of SnO₂ nanopowders. *Carbon* **2008**, *46*, 35-40.
147. Ng, S.H.; Wang, J.; Konstantinov, K.; Wexler, D.; Chen J.; Liu, H.K. Spray pyrolyzed PbO-carbon nanocomposites as anode for lithium-ion batteries. *J. Electrochem. Soc.* **2006**, *153*, A787-A797.
148. Ng, S.H.; Wang, J.; Wexler, D.; Chew S.Y.; Liu, H.K. Amorphous carbon-coated silicon nanocomposites: A low-temperature synthesis via spray pyrolysis and their application as high-capacity anodes for lithium-ion batteries. *J. Phys. Chem. C* **2007**, *111*, 11131-11138.
149. Du, N.; Zhang, H.; Chen, B.; Ma, X.Y.; Huang, X.H.; Tu, J.P.; Yang, D.R. Synthesis of polycrystalline SnO₂ nanotubes on carbon nanotube template for anode material of lithium-ion battery. *Mater. Res. Bull.* **2009**, *44*, 211-215.
150. Wang, Z.Y.; Chen, G.; Xia, D.G. Coating of multi-walled carbon nanotube with SnO₂ films of controlled thickness and its application for Li-ion battery. *J. Power Sources* **2008**, *184*, 432-436.
151. An, G.M.; Na, N.; Zhang, X.R.; Miao, Z.J.; Miao, S.D.; Ding, K.L.; Liu, Z.M. SnO₂/carbon nanotube nanocomposites synthesized in supercritical fluids: Highly efficient materials for use as a chemical sensor and as the anode of a lithium-ion battery. *Nanotechnology* **2007**, *18*, 435707:1-435707:6.
152. Qiao, H.; Zheng, Z.; Zhang, L.Z.; Xiao, L.F. SnO₂@C core-shell spheres: Synthesis, characterization, and performance in reversible Li-ion. *J. Mater. Sci.* **2008**, *43*, 2778-2784.
153. Lou, X.W.; Deng, D.; Lee, J.Y.; Archer, L.A. Preparation of SnO₂/carbon composite hollow spheres and their lithium storage properties. *Chem. Mater.* **2008**, *20*, 6562-6566.
154. Moon, T.; Kim, C.J.; Hwang, S.-T.; Park, B.W. Electrochemical properties of disordered-carbon-coated SnO₂ nanoparticles for Li rechargeable batteries. *Electrochem. Solid-State Lett.* **2006**, *9*, A408-A411.

155. Chen, M.H.; Huang, Z.C.; Wu, G.T.; Zhu, G.M.; You, J.K.; Lin, Z.G. Synthesis and characterization of SnO–carbon nanotube composite as anode material for lithium-ion batteries. *Mater. Res. Bull.* **2003**, *38*, 831-836.
156. Poizot, P.; Larulle, S.; Grugeon, S.; Dupont, L.; Tarascon, J.-M. Nano-sized transition-metal oxides as negative-electrode materials for lithium-ion batteries. *Nature* **2000**, *407*, 496-498.
157. Natarajan, C.; Setoguchi K.; Nogami, G. Preparation of a nanocrystalline titanium dioxide negative electrode for the rechargeable lithium ion battery. *Electrochem. Acta* **1998**, *43*, 3371-3374.
158. Ortiz, G.F.; Hanzu, I.; Djenizian, T.; Lavela, P.; Tirado, J.L.; Knauth, P. Alternative Li-ion battery electrode based on self-organized titania nanotubes. *Chem. Mater.* **2009**, *21*, 63-67.
159. Fu, L.J.; Liu, H.; Zhang, H.P.; Li, C.; Zhang, T.; Wu, Y.P.; Wu, H.Q. Novel TiO₂/C nanocomposites for anode materials of lithium ion batteries. *J. Power Sources* **2006**, *159*, 219-222.
160. Yoon, S.H.; Lee, C.; Park, M.; Oh, S.M. Preparation of nanotube TiO₂-carbon composite and its anode performance in lithium-ion batteries. *Electrochem. Solid-State Lett.* **2009**, *12*, A28-A32.
161. Fu, L.J.; Yang, L.C.; Shi, Y.; Wang, B.; Wu, Y.P. Synthesis of carbon coated nanoporous microcomposite and its rate capability for lithium ion battery. *Microporous Mesoporous Mater.* **2009**, *117*, 515-518.
162. Huang, X.H.; Tu, J.P.; Zhang, C.Q.; Xiang, J.Y. Net-structured NiO–C nanocomposite as Li-intercalation electrode material. *Electrochem. Commun.* **2007**, *9*, 1180-1184.
163. Huang, X.H.; Tu, J.P.; Zhang, C.Q.; Chen, X.T.; Yuan, Y.F.; Wu, H.M. Spherical NiO–C composite for anode material of lithium ion batteries. *Electrochimica Acta* **2007**, *52*, 4177-4181.
164. Yang, R.; Wang, Z.; Liu, J.; Chen, L. Nano Co₃O₄ particles embedded in porous hard carbon spherules as anode material for Li-ion batteries. *Electrochem. Solid-State Lett.* **2004**, *7*, A496-A499.
165. Liu, H.-J.; Bo, S.-H.; Cui, W.-J.; Li, F.; Wang, C.-X.; Xia, Y.-Y. Nano-sized cobalt oxide/mesoporous carbon sphere composites as negative electrode material for lithium-ion batteries. *Electrochim. Acta* **2008**, *53*, 6497-6503.
166. Li, H.; Zhu, G.Y.; Huang, X.J.; Chen, L.Q. Synthesis and electrochemical performance of dendrite-like nanosized SnSb alloy prepared by co-precipitation in alcohol solution at low temperature. *J. Mater. Chem.* **2000**, *10*, 693-696.
167. Li, H.; Shi, L.H.; Lu, W.; Huang, X.J.; Chen, L.Q. Studies on capacity loss and capacity fading of nanosized SnSb alloy anode for Li-ion batteries. *J. Electrochem. Soc.* **2001**, *148*, A915-A922.
168. Li, H.; Huang, X.J.; Chen, L.Q.; Zhou, G.W.; Zhang, Z.; Yu, D.P.; Mo, Y.J.; Pei, N. The crystal structural evolution of nano-Si anode caused by lithium insertion and extraction at room temperature. *Solid State Ionics* **2000**, *135*, 181-191.
169. Shi, L.H.; Li, H.; Wang, Z.X.; Huang, X.J.; Chen, L.Q. Nano-SnSb alloy deposited on MCMB as an anode material for lithium ion batteries. *J. Mater. Chem.* **2001**, *11*, 1502-1505.
170. Li, H.; Wang, Q.; Shi, L.H.; Chen, L.Q.; Huang, X.J. Nanosized SnSb alloy pinning on hard non-graphitic carbon spherules as anode materials for a Li ion battery. *Chem. Mater.* **2002**, *14*, 103-108.

171. Wang, Q.; Li, H.; Chen, L.Q.; Huang, X.J. Novel spherical microporous carbon as anode material for Li-ion batteries. *Solid State Ionics* **2002**, *152-153*, 43-50.
172. Wang, G.X.; Sun, L.; Bradhurst, D.H.; Zhong, S.; Dou, S.X.; Liu, H.K. Nanocrystalline NiSi alloy as an anode material for lithium-ion batteries. *J. Alloys Compd.* **2000**, *306*, 249-252.
173. Kim, I.-S.; Kumta, P.N.; Blomgren, G.E. Si/TiN nanocomposites novel anode materials for Li-ion batteries. *Electrochem. Solid-State Lett.* **2000**, *3*, 493-496.
174. Kang, Y.-M.; Park, M.-S.; Song, M.-S.; Han, Y.-S.; Lee, J.-Y. A relation between the electrochemical behaviors and morphology of Ni-Co₃O₄ composites prepared by the chemical reduction method or the mechanical milling. *Mater. Chem. Phys.* **2007**, *105*, 245-249.
175. Bazin, L.; Mitra, S.; Taberna, P.L.; Poizot, P.; Gressier, M.; Menu, M.J.; Barnabé, A.; Simon, P.; Tarascon, J.-M. High rate capability pure Sn-based nano-architected electrode assembly for rechargeable lithium batteries. *J. Power Sources* **2009**, *188*, 578-582.

© 2009 by the authors; licensee Molecular Diversity Preservation International, Basel, Switzerland. This article is an open-access article distributed under the terms and conditions of the Creative Commons Attribution license <http://creativecommons.org/licenses/by/3.0/>.